arXiv:2609.32740v1 [cs.CV] 26 Sep 2026

# ANESTRACE: BENCHMARKING INTRAOPERATIVE ANESTHESIA FROM MULTIMODAL PERCEPTION TO MULTI-STEP DECISION-MAKING

**Ziwei Huang**[1], **Qi Gao**[2], **Zhe Ji**[3,*], **Yuanyuan Yao**[2], **Fengjiang Zhang**[2], **Min Yan**[2✉]
**Zhongle Xie**[1✉], **Gang Chen**[1]

[1]School of Software Technology, Zhejiang University
[2]Department of Anesthesiology, The Second Affiliated Hospital of Zhejiang University School of Medicine
[3]School of Software, Central South University

## ABSTRACT

Intraoperative anesthesia requires systems to interpret evolving multimodal evidence, recommend timely management, and revise decisions as patient states change, yet existing benchmarks usually isolate perception or single-point reasoning. We introduce AnesTRACE, an evaluation suite comprising AnesTRACE-Bench and AnesTRACE-Eval. Built from public perioperative datasets with anesthesiologist annotation, AnesTRACE-Bench evaluates Intraoperative Perception, Single-point Anesthesia Decision-Making, and Multi-step Anesthesia Decision-Making. AnesTRACE-Eval assesses open-ended responses through anesthesiologist-defined criteria for Clinical Correctness, Evidence Grounding, Task Completeness, and Safety, with Temporal Consistency for multi-step decisions; its domain-specific evaluator is trained by supervised fine-tuning and preference alignment on expert-reviewed judgments. Across more than 30 models, fine-grained visual grounding and intervention selection remain difficult: the leading model reaches only 32.2 mIoU for TEE visual grounding and retains a 17.5% Major/Critical Safety Error Rate in multi-step management. Evaluator alignment with anesthesiologists improves across both training stages, while the best decision quality is accompanied by a 74.3-second P95 Latency. These results show that aggregate performance alone does not establish safe, timely longitudinal decision-making. We release our code at `https://github.com/zjuDBxAI/AnesTRACE`.

## 1 INTRODUCTION

Intraoperative anesthesia couples interpretation, intervention, and reassessment under changing physiological conditions, where delayed or inappropriate management can have immediate consequences (Nair et al., 2017; American Society of Anesthesiologists, 2025; Saugel et al., 2025). Anesthesiologists integrate heterogeneous signals, procedural context, ongoing treatment, and responses to prior interventions; the same physiological change can therefore require different management across intraoperative trajectories (Saugel et al., 2025). Medical AI intended for this setting must connect available evidence to management, update decisions over time, and respond within seconds.

Existing benchmarks cover complementary pieces of the process but not the complete intraoperative decision pathway. Knowledge benchmarks emphasize self-contained questions (Jin et al., 2021; Zuo et al., 2025; Singhal et al., 2023); multimodal benchmarks test interpretation without subsequent management (Hu et al., 2024; Oh et al., 2023); and agent or longitudinal benchmarks introduce tool use and evolving records outside repeated intraoperative management (Schmidgall et al., 2024; Jiang et al., 2025; Xu et al., 2026c). Anesthesiology benchmarks remain largely text-based and centered on specialty knowledge, consultation, or single-response clinical reasoning(Feng et al., 2026; Zhou et al., 2025). A shared testbed is therefore needed to separate perception, management reasoning, and decision updating while measuring response latency.

*Work done while at Zhejiang University.

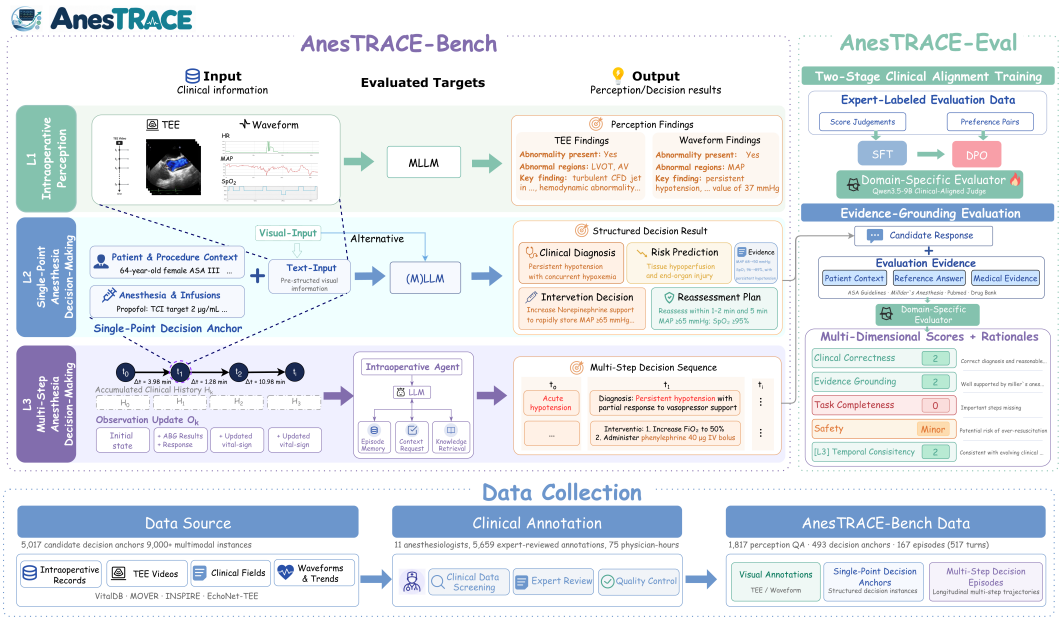


Figure 1: **Overview of AnesTRACE.** The bottom shows data collection and annotation, the upper left presents the three-level AnesTRACE-Bench task hierarchy, and the upper right shows the AnesTRACE-Eval framework.

Open-ended management also complicates evaluation because several plans may be acceptable, while consequential omissions or unsafe recommendations remain clinically important. Repeated anesthesiologist review is costly, whereas holistic LLM judging may overlook decision-time evidence, temporal dependencies, or safety failures (Arora et al., 2025; Bedi et al., 2025). Scalable evaluation consequently requires explicit evidence-grounded, temporal, and safety-sensitive criteria.

We introduce **AnesTRACE**, comprising *AnesTRACE-Bench* and *AnesTRACE-Eval* (Figure 1). Intraoperative practice requires different capabilities as clinicians move from interpreting monitoring data to selecting an intervention and reassessing it after the patient state changes. To reflect this workflow, AnesTRACE-Bench varies both the evaluated object and the information interface across **Intraoperative Perception (L1)**, **Single-point Anesthesia Decision-Making (L2)**, and **Multi-step Anesthesia Decision-Making (L3)**. Accordingly, L1 tests whether existing multimodal large language models (MLLMs) can extract findings from raw visual and physiological evidence, while L2 tests whether models can convert a standardized patient-state description into management at one decision time. L3 then places language models in a common agent framework to test information requests, memory, and management revision across successive decision points. The agents share bounded patient-information and knowledge tools, episode memory, and trajectory replay that reveals recorded states without allowing their proposals to alter the clinical trajectory. This controlled progression localizes whether a failure arises from perception, intervention reasoning, evidence acquisition, or longitudinal decision updating.

AnesTRACE-Eval addresses the aforementioned evaluation problem by translating anesthesiologist-defined atomic criteria into separate judgments for Clinical Correctness, Evidence Grounding, Task Completeness, and safety, while Temporal Consistency evaluates decision updating over an L3 episode. The criteria permit clinically acceptable alternatives, and safety remains separately reported so that unsafe recommendations are not obscured by stronger performance on other dimensions. A domain-specific evaluator learns this protocol through supervised fine-tuning and preference alignment on expert-reviewed judgments, enabling scalable evaluation while retaining explicit rationales for each applicable dimension.

Through benchmarking more than 30 models, we find that fine-grained perception and intervention selection remain weak, while the leading model retains a 17.5% L3 Safety Error Rate and requires 74.3 seconds for a full response for multi-step decisions, exceeding the 30-second operating-standard requirement. Clinical history, memory, and tools improve decision updating, while evaluator alignment with anesthesiologists improves after both training stages.

To summarize, our contributions are threefold:

- We introduce AnesTRACE-Bench, which diagnoses three complementary intraoperative capabilities by varying evidence representation, information access, and temporal scope within a shared clinical domain.
- We develop AnesTRACE-Eval, an anesthesiologist-aligned protocol and domain-specific evaluator for evidence-grounded, safety-sensitive, and temporally consistent assessment of open-ended management responses.
- We provide a systematic evaluation of 30 models and controlled analyses of the factors that shape clinical quality, latency, and evidence-acquisition cost across the three settings.

## 2 Related Work

**Perioperative Prediction and Clinical Decision-Making.** Perioperative AI has primarily targeted constrained prediction or control, including hypotension prediction (Hatib et al., 2018; Wijnberge et al., 2020), infusion adjustment (Miyaguchi et al., 2021), and closed-loop anesthetic administration (Puri et al., 2016; Pasin et al., 2017). These studies establish the value of perioperative signals but do not jointly test heterogeneous evidence integration, intervention selection, and decision updating.

**Anesthesiology Benchmarks and LLM-Based Evaluation.** CAB, Hypnos, and AnesSuite evaluate anesthesiology knowledge or reasoning through questions, consultations, and clinical scenarios (Zhou et al., 2025; Wang et al., 2025b; Feng et al., 2026). Other medical benchmarks separately cover multimodal perception (Hu et al., 2024; Oh et al., 2023), information gathering and EHR tools (Hager et al., 2024; Jiang et al., 2025), or evolving records (Xu et al., 2026c). AnesTRACE differs by separating raw-evidence perception, single-point management, and multi-step decision updating within one anesthesia-specific domain and controlled information interfaces.

For open-ended evaluation, Prometheus and JudgeLM train rubric-based evaluators (Kim et al., 2024; Zhu et al., 2025), while HealthBench and LLMEval-Med use physician-defined criteria and expert-validated judgments (Arora et al., 2025; Zhang et al., 2025). AnesTRACE-Eval extends criterion-based clinical evaluation to decision-time evidence, safety, and Temporal Consistency for intraoperative management. A comparison with related benchmarks and evaluators is summarized in Appendix B.

## 3 Task Formulation

AnesTRACE separates intraoperative perception, management reasoning, and decision updating through three complementary information settings.

### 3.1 Clinical State

For decision-oriented tasks, let $t_k$ denote the decision time associated with the $k$-th clinical decision anchor, a point at which the available evidence suggests a change in patient state that may warrant clinical reassessment or management adjustment. An anchor marks an opportunity for reassessment and does not require that a new intervention was recorded at that instant. A recent observation window selects dynamic measurements leading up to the decision:

$$W_k^{\text{obs}} = [t_k - \Delta_{\text{obs}}, t_k), \tag{1}$$

where $\Delta_{\text{obs}}$ is the predefined observation horizon. The patient state available at $t_k$ is represented as

$$S_k = \left(C,\, M_{t_k},\, O_{W_k^{\text{obs}}}\right), \tag{2}$$

where $C$ denotes patient and procedural context, $M_{t_k}$ denotes ongoing management, and $O_{W_k^{\text{obs}}}$ contains recent measurements and trends together with events and investigation results available by $t_k$. Inputs and patient-information tools expose only evidence available at the decision time; reference answers and screening labels remain hidden. Temporal alignment and filtering are detailed in Appendix A.1. We denote the initially supplied information by $I_k$, which may contain only part of $S_k$.

Table 1: Three-level task hierarchy of AnesTRACE-Bench, covering intraoperative perception, single-point management, and multi-step management.

| Level | Task | Input | Question | Response | Evaluation | Scale |
|---|---|---|---|---|---|---|
| L1 | TEE perception | TEE frames/videos | Option selection<br>Grounding<br>Open-ended | Option ID<br>Coordinates<br>Structured text | Accuracy<br>mIoU / F1 | 817 QA |
| | Waveform perception | Waveforms/trends | Option selection<br>Open-ended | Option ID(s)<br>Structured text | Accuracy<br>F1 | 1,000 QA |
| L2 | Single-point management | Clinical state $S_k$ | Open-ended | Structured text | AnesTRACE-Eval | 493 anchors |
| L3 | Multi-step management | State + history<br>$S_k$, $\mathcal{H}_k$ | Multi-turn | Structured text/turn | AnesTRACE-Eval | 167 episodes<br>517 turns |

### 3.2 Evaluation Task

**L1: Intraoperative Perception** maps a TEE frame or video, physiological waveform, or vital-sign trend plot and task prompt to an option, spatial localization, or structured clinical finding. Given raw input $x$ and prompt $q$, the model produces $\widehat{y} = f_\theta(x, q)$ as an option selection, spatial localization, or structured finding job out of 12 tasks (see Appendix B), without formulating a management recommendation.

**L2: Single-point Anesthesia Decision-Making** evaluates one management response $\widehat{A}_k = \pi_\theta(I_k, q_k)$ at the fixed decision time $T_0 = t_k$ from standardized textual evidence, without additional patient-information requests. In this expression, $q_k$ is the task prompt, $\pi_\theta$ is the evaluated model with parameters $\theta$, and $\widehat{A}_k$ is its assessment and management response. Prompts cover diagnosis, short-term risk, intervention selection, and reassessment planning.

**L3: Multi-step Anesthesia Decision-Making** evaluates information acquisition and decision updating by a language-model agent with bounded tools and episode memory. An episode $\mathcal{T}_i$ contains at least two decision points from recorded surgical case $i$:

$$\mathcal{T}_i = \left((t_{i,k}, S_{i,k}, A^{\text{rec}}_{i,k})\right)_{k=1}^{K_i}, \qquad K_i \geq 2. \tag{3}$$

Here $K_i$ is the number of decision points, $S_{i,k}$ is the patient state at decision time $t_{i,k}$, and $A^{\text{rec}}_{i,k}$ is a documented intervention when available. At decision point $k$, the agent starts from $I_k$ and may access history $\mathcal{H}_k$ and the permitted tool set $\mathcal{U}$ to produce retrieved information $R_k$ and a structured management response $\widehat{A}_k$:

$$(R_k, \widehat{A}_k) = \Pi_\theta(I_k, \mathcal{H}_k; \mathcal{U}), \tag{4}$$

$\Pi_\theta$ denotes the complete agent policy, including tool selection, memory access, and response generation by the underlying model. Tools expose only information available at $t_k$, and memory distinguishes agent proposals from recorded interventions. After submission, trajectory replay reveals the next recorded state and intervention outcome; note that $\widehat{A}_k$ does not alter the trajectory.

**Design Rationale and Clinical Usefulness.** The three protocols mirror distinct requirements of intraoperative care: extracting findings from heterogeneous monitoring data, converting an available patient state into an immediate management plan, and reassessing that plan after the state or documented treatment response changes. Keeping these interfaces separate is clinically meaningful because an incorrect recommendation may originate from missed evidence, faulty management reasoning, or failure to incorporate temporal context, each of which calls for a different improvement strategy. The design is also operationally useful: standardized L2 inputs permit controlled comparison of management reasoning, while bounded L3 tools and trajectory replay test information-seeking and decision continuity without exposing future records or claiming to simulate the physiological effects of model-proposed actions.

## 4 AnesTRACE-Bench

**Overall Design.** Figure 1 summarizes the three task settings and their controlled information interfaces. Task-specific metrics assess L1, while AnesTRACE-Eval assesses L2 and L3 responses and adds episode-level Temporal Consistency for L3 (Section 5). Controlled comparisons vary input

Table 2: Evaluation dimensions, values, and applicable units in AnesTRACE-Eval.

| Dimension | Assessment | Values | Evaluation unit |
|---|---|---|---|
| Clinical Correctness | Clinical conclusions and management | 0, 1, 2 | L2 response; L3 decision turn |
| Evidence Grounding | Support from available evidence | 0, 1, 2 | L2 response; L3 decision turn |
| Task Completeness | Coverage of requested content | 0, 1, 2 | L2 response; L3 decision turn |
| Temporal Consistency | Decision updating as evidence evolves | 0, 1, 2 | Complete L3 episode |
| Safety | Unsafe actions, consequential omissions, and inappropriate clinical delays | *safe*, *minor*, *major*, *critical* | L2 intervention and reassessment outputs; L3 intervention decisions |

representation, clinical history, memory, and tool access; Appendix D.3 provides configurations and budgets. This organization does not assume that success at one level implies success at the next; instead, it makes distinct failure sources observable within a common clinical domain.

**Data Curation.** We draw on VitalDB (Lee et al., 2022) and MOVER (Samad et al., 2023) for perioperative records and physiological measurements, INSPIRE (Lim et al., 2024) for structured perioperative records, and EchoNet-TEE (Steffner et al., 2024) for TEE material. Dataset-specific parsers harmonize context, management, observations, units, and relative timestamps; records with unreliable alignment, insufficient evidence, or unresolved artifacts are excluded. Perception questions are constructed from selected TEE and physiological inputs, while candidate clinical decision anchors are identified from clinically meaningful changes, procedural phases, and newly available results. Expert-informed rules account for contexts such as cardiopulmonary bypass and deep hypothermic circulatory arrest, in which ordinary physiological thresholds may not indicate the same clinical state. The initial pool contains 5,017 candidate clinical decision anchors and more than 9,000 multimodal instances. A retained anchor supplies an L2 decision point; ordered anchors form L3 episodes with future states withheld. L2 therefore isolates one decision from evidence available at a fixed time, whereas L3 reveals later states and documented intervention outcomes only after each agent response. Appendix A.1 details source alignment and inclusion criteria.

**Expert Review and Quality Guarantee.** An open-source language model assists candidate generation, after which anesthesiologists review clinical relevance, correctness, decision-time evidence, anchor validity, and evidence sufficiency. Reference responses permit clinically acceptable alternatives and identify consequential errors. Temporal validation removes cases whose reference response relies on information that became available only after the relevant decision time. Appendix A.4 details annotation and temporal validation.

After expert review, L1 contains 817 TEE and 1,000 waveform or trend question–answer instances; L2 contains 493 clinical decision anchors from 467 surgical cases; and L3 contains 167 episodes comprising 517 turns from 124 surgical cases. These units are reported separately because questions, anchors, episodes, and turns are not interchangeable; Appendix B.1 provides task definitions, formats, counts, and metrics. The retrospective design and selected episodes limit extrapolation to unrepresented settings and to outcomes from executing model recommendations.

## 5 AnesTRACE-Eval

AnesTRACE-Eval combines an anesthesiologist-defined clinical protocol with a domain-specific evaluator for L2 and L3 responses, extending criterion-based medical evaluation with decision-time evidence and temporal assessment (Arora et al., 2025; Bedi et al., 2025; Zhang et al., 2025).

**Criterion-Based Clinical Evaluation.** As shown in Figure 1, AnesTRACE-Eval combines a candidate response with three groups of evaluation evidence: patient context, a reference answer, and medical evidence. For L2, patient context contains the information available at the decision point; for L3, it additionally contains the episode history of patient states, agent recommendations, and documented interventions. Patient context establishes the case facts, the reference answer describes

an expert-supported response without defining the only acceptable plan, and authoritative anesthesiology, ASA, and pharmacological sources support clinical interpretation (Gropper et al., 2024; American Society of Anesthesiologists, 2025; Knox et al., 2024). Atomic criteria specify the clinical requirements applicable to a case without forcing one reference wording or one acceptable management plan. The evaluator jointly assigns dimension-level judgments because individual criteria provide evidence for the response-level clinical assessment rather than independent benchmark scores.

Given input $x$, evaluator $J_\phi$ jointly produces applicable dimension-level judgments and rationales:

$$J_\phi(x) = \left\{(s_d, r_d)\right\}_{d \in \mathcal{D}(x)}, \tag{5}$$

Here $\mathcal{D}(x)$ contains the applicable dimensions and $(s_d, r_d)$ pairs each judgment with its rationale (Table 2).

For L3, Temporal Consistency is assessed once per episode by whether recommendations are maintained or revised appropriately as evidence evolves. This episode-level judgment complements turn-level Clinical Correctness, Evidence Grounding, and Task Completeness by testing whether later decisions incorporate newly revealed states and documented intervention outcomes.

Ordinal scores are averaged over their response-, turn-, or episode-level units. Safety is reported separately for applicable L2 and L3 outputs as the Major/Critical Safety Error Rate:

$$\text{Safety Error} = \frac{1}{N} \sum_{k=1}^{N} \mathbb{I}[s_{\text{saf},k} \in \{\textit{major}, \textit{critical}\}], \tag{6}$$

Here $N$ counts applicable outputs with valid safety labels. Safety remains separate from average clinical scores, and Appendix B provides the complete rubrics and aggregation rules. Separating safety prevents a low-frequency but consequential unsafe action or omission from disappearing inside an average of more common clinical judgments.

**Anesthesiologist-Aligned Evaluator Training.** We train the domain-specific evaluator as a companion to AnesTRACE-Bench using supervision derived from benchmark cases. DeepSeek-V4-Pro (Xu et al., 2026a) generates response variants, judgments, rationales, and preference pairs, which anesthesiologists correct and rank. Starting from Qwen3.5-9B, supervised fine-tuning uses approximately 7,000 expert-reviewed examples, followed by Direct Preference Optimization on approximately 4,000 expert-ranked pairs (Rafailov et al., 2023). Each response-level SFT example contains the judgments and rationales for all applicable dimensions, while a trajectory-level example is counted once per episode rather than once per turn or criterion. Appendix C provides annotation and optimization details.

Because evaluator-training cases overlap with benchmark cases by design, validation measures agreement with anesthesiologists on benchmark responses and does not establish generalization to unseen clinical cases. Section 6 compares base, SFT-only, and preference-aligned variants on 100 L2 responses and 117 L3 decision-turn responses reviewed by three anesthesiologists.

# 6 Experiments

## 6.1 Experimental Setup

**Baselines and Evaluation Protocols.** We evaluate more than 30 proprietary, general-purpose open-weight, and medical-domain models (Bai et al., 2025; Wang et al., 2025a; Li et al., 2024; Qwen Team, 2026b; Yang et al., 2025; Zeng et al., 2025a; Guo et al., 2025; Agarwal et al., 2025; Xu et al., 2026b; Liu et al., 2025; Zhang et al., 2023; Dou et al., 2025; Sellergren et al., 2025; Feng et al., 2026). Note that we vary model size because real-world hospitals face finite local compute (De Man et al., 2014; Wijnberge et al., 2020), and report latency because high-quality responses may still be unusable outside the clinical response window[1]. L1 uses raw visual inputs, L2 uses standardized textual evidence, and L3 uses a shared agent framework with episode memory and bounded tools; Appendix E provides complete settings. For open-ended L1 responses, Factual F1 and Metric-F1 match extracted clinical triplets against anesthesiologist-annotated references; L2 and L3 use AnesTRACE-Eval presented in Section 5.

[1]We set it 30 seconds indicated by our anesthesiologist collaborator.

Table 3: Performance of variant MLLMs on the intraoperative perception tasks of AnesTRACE-Bench. Bold indicates the best result in each column. Background colors denote model size: Small ($< 10$B), Medium (10–40B), and Large ($> 40$B).

| | Model | TEE | | | | | Waveform | | |
|---|---|---|---|---|---|---|---|---|---|
| | | Foundational Perception | Visual Grounding | | Functional Assessment | | Value Extraction | Trend Reasoning | Anomaly Perception |
| | | ACC | ACC | mIoU | ACC | Factual-F1 | ACC | Set-F1 | Metric-F1 |
| Proprietary MLLMs | GPT-6-Astra | 73.9 | **62.9** | **32.2** | 40.6 | 27.5 | **91.5** | 61.1 | **64.8** |
| | Gemini 3 Pro Preview | 71.6 | 46.1 | 24.6 | 34.4 | 23.7 | 77.0 | 62.6 | 54.8 |
| | Claude-Fable-5 | **74.5** | 42.7 | 23.4 | 37.8 | 26.9 | 80.5 | 68.7 | 59.6 |
| General Open-Weight MLLMs | Qwen3.8-MAX | 73.2 | 51.7 | 22.8 | **48.2** | **29.9** | 72.0 | 69.6 | 42.8 |
| | Qwen3.8-27B | 58.5 | 33.7 | 14.8 | 44.5 | 14.0 | 57.5 | **72.5** | 31.3 |
| | Qwen3.5-27B | 58.5 | 43.8 | 18.9 | 43.2 | 16.5 | 56.0 | 65.3 | 36.5 |
| | Qwen3.5-9B | 54.2 | 52.8 | 15.5 | 42.0 | 8.7 | 54.5 | 60.7 | 33.1 |
| | Qwen3-VL-8B | 51.5 | 23.6 | 14.4 | 35.6 | 5.7 | 45.0 | 58.2 | 23.5 |
| | LLaVA-OneVision-2-8B | 49.9 | 50.6 | 14.3 | 37.1 | 9.7 | 49.5 | 60.6 | 23.6 |
| | InternVL3.5-8B | 54.0 | 48.3 | 13.9 | 34.8 | 6.3 | 41.0 | 70.1 | 17.3 |
| Medical-Domain Open-Weight MLLMs | Fleming-VL-38B | 50.3 | 37.1 | 14.8 | 28.2 | 11.2 | 41.5 | 59.4 | 24.0 |
| | Lingshu-32B | 55.0 | 46.1 | 12.1 | 35.2 | 17.6 | 49.5 | 64.6 | 20.0 |
| | Lingshu-I-8B | 53.5 | 56.2 | 13.5 | 33.4 | 9.2 | 39.0 | 59.5 | 23.3 |
| | Fleming-VL-8B | 47.2 | 46.1 | 8.7 | 12.9 | 7.3 | 38.5 | 41.1 | 17.6 |

Table 4: Performance of variant LLMs on the decision-making tasks of AnesTRACE-Bench. Higher is better except for Safety Error and latency; bold indicates the best result in each column. Background colors denote model size: Small ($< 10$B), Medium (10–40B), and Large ($> 40$B).

| | Model | Single-Point Decision Making | | | | | | | Multi-Step Decision Making | | | | |
|---|---|---|---|---|---|---|---|---|---|---|---|---|---|
| | | Risk↑ | Diagnosis↑ | Intervention↑ | Reassessment↑ | Avg.↑ | Safety Error↓ | P95 Latency (s)↓ | Turn-level Avg.↑ | Temporal Consistency↑ | Safety Error↓ | Evidence Acquisition↑ | P95 Latency (s)↓ |
| Proprietary LLMs | GPT-6-Astra | 80.8 | **93.7** | **96.0** | **98.4** | **92.2** | **3.4** | 33.41 | **82.7** | **87.6** | **17.5** | 61.8 | 74.3 |
| | Gemini 3 Pro Preview | 71.1 | 74.7 | 68.9 | 86.1 | 75.2 | 13.5 | 26.95 | 66.1 | 78.0 | 38.5 | 74.4 | 101.4 |
| | Claude-Fable-5 | **87.1** | 91.9 | 87.8 | 96.3 | 90.8 | 9.4 | 39.96 | 79.4 | 82.5 | 24.3 | 84.4 | 69.2 |
| General Open-Weight LLMs | DeepSeek-V4-Pro | 78.2 | 83.5 | 79.0 | 93.8 | 83.6 | 14.8 | 14.04 | 80.0 | 81.9 | 19.2 | 89.7 | 14.4 |
| | Qwen3.8-Max | 70.7 | 79.6 | 71.6 | 87.5 | 77.4 | 15.1 | 23.51 | 67.1 | 85.3 | 40.1 | 62.8 | 22.9 |
| | Qwen3.5-27B | 69.4 | 74.6 | 70.2 | 77.9 | 73.0 | 28.6 | 22.14 | 69.5 | 81.6 | 32.5 | 83.3 | 34.4 |
| | Qwen3.8-27B | 71.4 | 75.5 | 66.1 | 75.0 | 72.0 | 21.5 | 22.94 | 66.1 | 69.2 | 34.1 | 86.9 | 39.9 |
| | GPT-OSS-20B | 69.1 | 65.8 | 50.7 | 66.1 | 62.9 | 37.5 | 17.90 | 57.1 | 67.2 | 53.4 | 59.5 | 106.6 |
| | GLM-4.7-Flash | 58.5 | 58.6 | 46.1 | 59.7 | 55.7 | 48.2 | 36.62 | 44.1 | 49.9 | 70.8 | 95.4 | 63.6 |
| | Qwen3.5-9B | 65.3 | 70.0 | 57.0 | 71.9 | 66.1 | 27.7 | 15.18 | 55.1 | 64.2 | 61.9 | 89.5 | 27.2 |
| | Qwen3-8B | 58.2 | 52.2 | 37.6 | 50.8 | 49.7 | 57.6 | 24.50 | 30.2 | 45.2 | 64.1 | 32.7 | **10.3** |
| Medical-Domain Open-Weight LLMs | Morpheus-32B | 55.0 | 50.4 | 41.7 | 58.0 | 51.3 | 56.9 | 20.31 | 46.2 | 56.0 | 66.0 | 67.5 | 86.9 |
| | Fleming-R1-32B | 63.9 | 63.9 | 46.4 | 67.0 | 60.3 | 37.6 | 14.55 | 52.8 | 66.9 | 56.5 | 11.3 | 22.8 |
| | HuatuoGPT-3-32B | 62.7 | 60.7 | 47.6 | 59.7 | 57.7 | 50.9 | 25.05 | 49.9 | 61.7 | 64.7 | 73.4 | 31.3 |
| | Baichuan-M2-32B | 57.9 | 62.0 | 48.2 | 51.5 | 54.9 | 42.1 | 75.10 | 49.5 | 56.1 | 66.7 | **96.0** | 33.0 |
| | MedGemma-27B-text-it | 64.7 | 61.2 | 41.5 | 63.3 | 57.7 | 43.7 | 12.44 | 48.7 | 54.3 | 59.4 | 40.5 | 34.4 |
| | HuatuoGPT-3-8B | 44.3 | 38.8 | 35.6 | 45.5 | 41.1 | 85.9 | 9.87 | 33.8 | 48.2 | 86.6 | 29.1 | 99.9 |
| | Morpheus-7B | 47.0 | 42.3 | 39.0 | 50.4 | 44.7 | 67.4 | 26.80 | 35.1 | 46.7 | 78.2 | 8.3 | 50.4 |
| | Fleming-R1-7B | 55.0 | 52.5 | 40.5 | 55.2 | 50.8 | 59.0 | **9.19** | 44.5 | 56.6 | 69.4 | 4.6 | 33.1 |

### 6.2 Main Results on AnesTRACE

**From recognition to clinically usable perception.** Table 3 shows that strong basic recognition does not extend uniformly to fine-grained intraoperative interpretation. GPT-6-Astra reaches 32.2 mIoU for TEE grounding and 27.5 Factual-F1 for functional assessment, while the best waveform anomaly Metric-F1 is 64.8, indicating that *fine-grained evidence extraction is one of the primary perception bottlenecks*. For clinical use, the result means that model-derived findings should remain linked to localized source evidence before they inform intraoperative management.

**From patient state to safe sequential management.** Table 4 shows that intervention selection trails overall L2 performance for most models, including GPT-OSS-20B (50.7 versus 62.9) and MedGemma-27B-text-it (41.5 versus 57.7). Standardized evidence therefore reduces variation in perception but *does not resolve the challenge of converting the patient state and ongoing manage-*

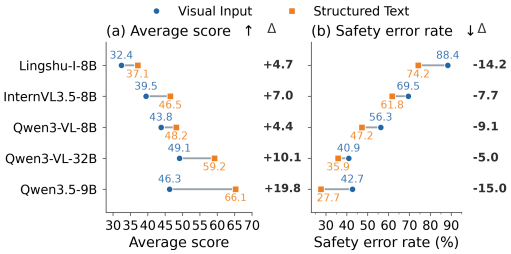


Figure 2: Effect of input representation ablation for five MLLMs on L2 tasks. Δ denotes structured text minus visual input.

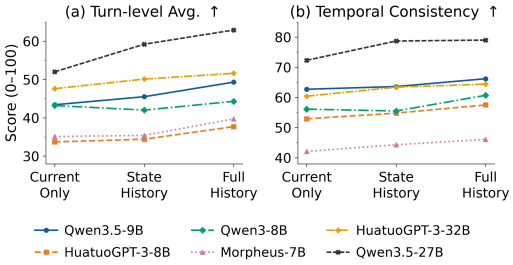


Figure 3: Clinical-history ablation. Avg. averages correctness, grounding, and completeness.

Table 5: Comparison of AnesTRACE-Eval variants in agreement with anesthesiologist ratings. Each cell reports L2/L3. Spear. and Kend. denote Spearman's $\rho$ and Kendall's $\tau_b$, respectively.

| Dimension | Base | | SFT | | SFT + DPO | |
|---|---|---|---|---|---|---|
| | Spear. | Kend. | Spear. | Kend. | Spear. | Kend. |
| **Correct.** | .46/.48 | .43/.44 | .57/.68 | .53/.63 | **.60/.71** | **.56/.66** |
| **Grounding** | .44/.35 | .41/.32 | .48/.66 | .45/.62 | **.52/.69** | **.49/.65** |
| **Complete.** | .39/.45 | .32/.38 | .50/.46 | .47/.42 | **.59/.68** | **.54/.63** |
| **Total** | .49/.47 | .42/.39 | .53/.72 | .45/.62 | **.58/.75** | **.50/.65** |
| **Safety** | .38/.47 | .34/.41 | .48/.77 | .43/.70 | **.51/.80** | **.47/.73** |
| **Temporal** | –/.37 | –/.34 | –/.55 | –/.52 | **–/.58** | **–/.55** |

Table 6: Effect of agent components on multi-step anesthesia decision-making with Qwen3.5-27B.

| Method | Avg.↑ | Temporal Consistency↑ | Safety Error↓ |
|---|---|---|---|
| Full Agent | 69.1 | 81.6 | 32.5 |
| w/o Memory | 63.8 | 67.5 | 35.3 |
| w/o Knowledge Tools | 63.2 | 80.5 | 43.8 |
| w/o Clinical Requests | 48.7 | 79.2 | 54.3 |
| w/o All Tools | 37.9 | 64.8 | 57.4 |

*ment into an appropriate action*. In L3, GPT-6-Astra leads Turn-level Avg., Temporal Consistency, and Safety, whereas medical-domain open-weight models show no consistent advantage: Fleming-R1-32B reaches 52.8 in Turn-level Avg. versus 69.5 for Qwen3.5-27B. Safety errors increase from 3.4% to 17.5% for GPT-6-Astra and from 9.4% to 24.3% for Claude-Fable-5 between L2 and L3, showing that *strong individual decisions do not ensure safe management across a trajectory*.

**Technical and clinical implications.** Across the three settings, the principal technical bottleneck shifts from fine-grained evidence extraction to intervention selection and then to safe decision updating. These shifts indicate that *reliable intraoperative support requires joint gains in perception, reasoning, safety, and efficiency*. For clinical use, the results indicate that current models should support anesthesiologists by presenting traceable evidence and updated recommendations under human oversight; aggregate quality alone is insufficient for entrusting AI with independent intraoperative management. Appendix F provides full dimension-wise, subgroup, efficiency, and error analyses.

### 6.3 Ablation and Clinical Alignment

**Impact of Input Representation on Decision-Making.** Across five MLLMs, replacing visual waveform or trend inputs with matched structured text improves L2 Avg. and reduces Safety Error in Figure 2; Qwen3.5-9B changes from 46.3 to 66.1 and from 42.7% to 27.7%, respectively. Because the paired inputs hold the clinical case fixed, the improvement isolates the burden of visual evidence extraction; the remaining 27.7–74.2% Safety Error shows that *structured inputs reduce the perception burden but do not resolve unsafe management reasoning*. In practice, structured summaries may improve decision support when raw-signal interpretation is unreliable, but clinically useful systems must preserve source evidence and jointly validate both perception and the resulting intervention.

**Ablation on Clinical History, Tools, and Episode Memory.** Full History yields the highest Turn-level Avg. and Temporal Consistency across all six models (Figure 3); for Qwen3.5-27B, these rise from 52.0 to 62.9 and from 72.3 to 79.0 over Current Only. In the separate agent-component configuration of Table 6, removing memory lowers Temporal Consistency from 81.6 to 67.5, removing clinical requests lowers Turn-level Avg. from 69.1 to 48.7, and removing knowledge tools raises Safety Error from 32.5% to 43.8%. Together, these results show that *history, memory, and tool access make distinct contributions to decision updating*. Clinically, an intraoperative assistant must retain prior actions and responses, request missing patient information, and retrieve relevant knowledge so that each recommendation remains connected to the evolving case.

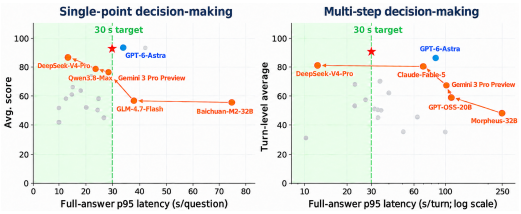


Figure 4: Quality–latency landscape for decision-making tasks. Dots represent evaluated models, orange arrows indicate ideal improvement scenarios, and red stars mark hypothetical operating points at the 30-second target.

**Alignment of AnesTRACE-Eval with Anesthesiologists.** Three anesthesiologists reviewed 100 L2 responses and 117 L3 decision-turn responses from 39 episodes; from the base model to SFT+DPO, total-score Spearman correlation rises from .49 to .58 in L2 and from .47 to .75 in L3, while L3 Safety Error correlation rises from .47 to .80 (Table 5). Together, these gains show that *task-specific SFT and DPO improve alignment with anesthesiologists across all evaluated dimensions*. Clinically, this agreement supports scalable screening and comparison of model responses, while the remaining disagreement requires anesthesiologist review for safety-critical interpretation; Appendix C.3 details annotation and aggregation.

**Decision Quality and Inference Efficiency.** Figure 4 shows that GPT-6-Astra attains an L3 Turn-level Avg. of 82.7 at 74.3 seconds, whereas DeepSeek-V4-Pro reaches 80.0 at 14.4 seconds; the red star marks the hypothetical combination of the best observed quality and the 30-second operating-room deployment requirement. This comparison shows that *inference efficiency is an independent requirement for clinical deployment*. For time-sensitive intraoperative deterioration, systems must return useful evidence and recommendations within the clinical response window (De Man et al., 2014; Wijnberge et al., 2020); meeting that window still does not establish safety and therefore cannot replace prospective clinical validation and anesthesiologist oversight.

### 6.4 Hospital-oriented model selection

Applying the preceding production criteria changes how the results should be used: externally hosted models, such as GPT-6-Astra and Claude-Fable-5, define a capability reference, whereas local candidates must jointly satisfy quality, safety, latency, and resource constraints.

Under these constraints, Qwen3.5-9B is the most practical starting point among the evaluated locally deployed general-purpose models: its 9B scale and 27.2-second L3 latency accompany a 55.1 Turn-level Avg. and 89.5 Evidence Acquisition. AnesTRACE supports this choice by mapping the intended role to L1–L3, applying deployment gates, and using controlled comparisons to decide whether perception, episode memory, patient-information requests, or knowledge retrieval should be added to the agent. However, its 61.9% L3 Safety Error and moderate decision quality show that this choice still remains *far from patient-care readiness*, and *no evaluated local model simultaneously satisfies* the desired quality, safety, latency, and resource profile. Nonetheless, the benchmark defines both a current selection frontier and a measurable development path toward efficient, clinically grounded agents with abstention, escalation, and prospective validation under anesthesiologist oversight.

## 7 Conclusion

To address the lack of a shared testbed that connects multimodal evidence interpretation, intervention selection, and longitudinal decision-making, we introduce AnesTRACE, comprising AnesTRACE-Bench and AnesTRACE-Eval, in this paper. AnesTRACE-Bench evaluates Intraoperative Perception, Single-point Anesthesia Decision-Making, and Multi-step Anesthesia Decision-Making, while AnesTRACE-Eval provides anesthesiologist-aligned assessment of open-ended responses across grounding, temporal consistency, and safety. Across more than 30 models, results expose persistent gaps in fine-grained perception and intervention selection; even the leading model retains a 17.5% Safety Error and requires 74.3 seconds. AnesTRACE therefore provides the field with a clinically structured diagnostic framework for identifying where current systems fail and for guiding the development of evidence-grounded, efficient, and clinician-supervised intraoperative support. Future work could separate evaluator training from external validation, extend coverage of rare and high-risk scenarios, and prospectively study workflow integration without treating retrospective benchmark performance as evidence of readiness for patient care.

## AI USE STATEMENT

In this work, we used generative AI tools to assist benchmark construction, generate candidate responses for expert annotation, and support the training and application of AnesTRACE-Eval. LLMs also served as evaluated systems. Additionally, we used generative AI tools for proofreading, sentence refinement, and improving linguistic clarity. These constitute all uses of generative AI in this work. AI-assisted manuscript revisions were reviewed and edited by the authors, and model-assisted annotation materials were reviewed by anesthesiologists. Details of model use and annotation procedures are provided in the corresponding sections of the main text and appendix. We take responsibility for the final content of this work, including text, claims, and artifacts produced with the aid of generative AI.

## ETHICS STATEMENT

AnesTRACE is constructed from retrospective, de-identified records obtained from the VitalDB, MOVER, INSPIRE, and EchoNet-TEE research datasets. We collected no new patient data and had no interaction with patients. The benchmark retains only de-identified source identifiers and relative timestamps. We respected source access restrictions, made no attempt to re-identify individuals, and do not redistribute restricted raw records, cross-dataset linkage tables, or licensed reference materials. All experiments were conducted retrospectively, and no model output informed patient care. AnesTRACE is intended for research evaluation and does not establish clinical readiness: model responses may contain unsafe recommendations or consequential omissions. Any downstream use must respect patient privacy and applicable dataset licenses; clinical use would require appropriate validation and qualified human oversight.

## REPRODUCIBILITY STATEMENT

We provide anonymous code for decision-anchor construction, preprocessing of TEE videos, physiological waveforms, and vital-sign trends, benchmark inference and evaluation, and AnesTRACE-Eval training. The main text and appendix describe data curation and annotation, task definitions, evaluation metrics, model configurations, and evaluator training. Upon acceptance, we will release all AnesTRACE-Bench datasets and AnesTRACE-Eval checkpoints, subject to applicable data licenses and access requirements. Access to restricted source data must be obtained from the respective providers. The code is available at `https://anonymous.4open.science/r/AnesTRACE-027C/`.

## REFERENCES


Sandhini Agarwal, Lama Ahmad, Jason Ai, Sam Altman, Andy Applebaum, Edwin Arbus, Rahul K Arora, Yu Bai, Bowen Baker, Haiming Bao, et al. gpt-oss-120b & gpt-oss-20b model card. *arXiv preprint arXiv:2508.10925*, 2025.

Alibaba Cloud. Alibaba unveils Qwen3.8-Max, 2026. URL `https://www.alibabacloud.com/en/press-room/alibaba-unveils-qwen3-8-max`.

American Society of Anesthesiologists. Standards for basic anesthetic monitoring. American Society of Anesthesiologists, 2025. Last amended October 15, 2025.

Anthropic. Claude fable 5 and claude mythos 5, 2026. URL `https://www.anthropic.com/news/claude-fable-5-mythos-5`.

Rahul K Arora, Jason Wei, Rebecca Soskin Hicks, Preston Bowman, Joaquin Quiñonero-Candela, Foivos Tsimpourlas, Michael Sharman, Meghan Shah, Andrea Vallone, Alex Beutel, et al. Healthbench: Evaluating large language models towards improved human health. *arXiv preprint arXiv:2505.08775*, 2025.

Shuai Bai, Yuxuan Cai, Ruizhe Chen, Keqin Chen, Xionghui Chen, Zesen Cheng, Lianghao Deng, Wei Ding, Chang Gao, Chunjiang Ge, et al. Qwen3-vl technical report. *arXiv preprint arXiv:2511.21631*, 2025.

Suhana Bedi, Hejie Cui, Miguel Fuentes, Alyssa Unell, Michael Wornow, Juan M Banda, Nikesh Kotecha, Timothy Keyes, Yifan Mai, Mert Oez, et al. Medhelm: Holistic evaluation of large language models for medical tasks. *arXiv preprint arXiv:2505.23802*, 2025.

Julie PW Bynum, Laura Barre, Catherine Reed, and Honor Passow. Participation of very old adults in health care decisions. *Medical decision making*, 34(2):216–230, 2014.

Junying Chen, Xinyuan Xie, Ziniu Li, and Benyou Wang. OnePO: Direct one-stage policy optimization for SFT-free domain adaptation. In *Proceedings of the 43rd International Conference on Machine Learning*, 2026.

Pengcheng Chen, Jin Ye, Guoan Wang, et al. Gmai-mmbench: A comprehensive multimodal evaluation benchmark towards general medical ai. In *Advances in Neural Information Processing Systems*, 2024. URL https://proceedings.neurips.cc/paper_files/paper/2024/hash/ab7e02fd60e47e2a379d567f6b54f04e-Abstract-Datasets_and_Benchmarks_Track.html.

Martin D Culwick, Yasmin Endlich, and Stavros N Prineas. The bowtie diagram: a simple tool for analysis and planning in anesthesia. *Current Opinion in Anaesthesiology*, 33(6):808, 2020.

FR De Man, M Erwteman, D van Groeningen, PV Ziedses des Plantes, C Boer, SA Loer, and R Krage. The effect of audible alarms on anaesthesiologists' response times to adverse events in a simulated anaesthesia environment: a randomised trial. *Anaesthesia*, 69(6):598–603, 2014.

DeepSeek. DeepSeek-V4 preview: Entering the era of affordable million-token context, 2026. URL https://deepseek.com/en/news/v4-preview/.

Chengfeng Dou, Chong Liu, Fan Yang, Fei Li, Jiyuan Jia, Mingyang Chen, Qiang Ju, Shuai Wang, Shunya Dang, Tianpeng Li, et al. Baichuan-m2: Scaling medical capability with large verifier system. *arXiv preprint arXiv:2509.02208*, 2025.

Xiang Feng, Wentao Jiang, Zengmao Wang, Yong Luo, Pingbo Xu, Baosheng Yu, Hua Jin, and Jing Zhang. Anessuite: a comprehensive benchmark and dataset suite for anesthesiology reasoning in llms. In *International Conference on Learning Representations*, volume 2026, pp. 141654–141700, 2026.

Google. Gemini 3 Pro Preview model documentation, 2025. URL https://ai.google.dev/gemini-api/docs/models/gemini-3-pro-preview.

Michael A. Gropper, Lars I. Eriksson, Lee A. Fleisher, Neal H. Cohen, Kate Leslie, and Oluwaseun Johnson-Akeju (eds.). *Miller's Anesthesia*. Elsevier, 10 edition, 2024. ISBN 9780323935920.

Daya Guo, Dejian Yang, Haowei Zhang, Junxiao Song, Peiyi Wang, Qihao Zhu, Runxin Xu, Ruoyu Zhang, Shirong Ma, Xiao Bi, et al. Deepseek-r1: Incentivizing reasoning capability in llms via reinforcement learning. *arXiv preprint arXiv:2501.12948*, 2025.

Paul Hager, Friederike Jungmann, Robbie Holland, et al. Evaluation and mitigation of the limitations of large language models in clinical decision-making. *Nature Medicine*, 30:2613–2622, 2024. doi: 10.1038/s41591-024-03097-1.

Feras Hatib, Zhongping Jian, Sai Buddi, Christine Lee, Jos Settels, Karen Sibert, Joseph Rinehart, and Maxime Cannesson. Machine-learning algorithm to predict hypotension based on high-fidelity arterial pressure waveform analysis. *Anesthesiology*, 129(4):663–674, 2018.

Yutao Hu, Tianbin Li, Quanfeng Lu, Wenqi Shao, Junjun He, Yu Qiao, and Ping Luo. Omnimedvqa: A new large-scale comprehensive evaluation benchmark for medical lvlm. In *2024 IEEE/CVF Conference on Computer Vision and Pattern Recognition (CVPR)*, pp. 22170–22183. IEEE, 2024.

Yixing Jiang, Kameron C Black, Gloria Geng, Danny Park, James Zou, Andrew Y Ng, and Jonathan H Chen. Medagentbench: a virtual ehr environment to benchmark medical llm agents. *Nejm Ai*, 2(9):AIdbp2500144, 2025.

Di Jin, Eileen Pan, Nassim Oufattole, Wei-Hung Weng, Hanyi Fang, and Peter Szolovits. What disease does this patient have? a large-scale open domain question answering dataset from medical exams. *Applied Sciences*, 11(14):6421, 2021.

Maurice G Kendall. The treatment of ties in ranking problems. *Biometrika*, 33(3):239–251, 1945.

Seungone Kim, Jay Shin, Joel Jang, Shayne Longpre, Hwaran Lee, Sangdoo Yun, Ryan Shin, Sungdong Kim, James Thorne, Minjoon Seo, et al. Prometheus: Inducing fine-grained evaluation capability in language models. In *International Conference on Learning Representations*, volume 2024, pp. 29927–29962, 2024.

Craig Knox, Michael Wilson, Colin M. Klinger, et al. Drugbank 6.0: the drugbank knowledgebase for 2024. *Nucleic Acids Research*, 52(D1):D1265–D1275, 2024. doi: 10.1093/nar/gkad976.

LangChain AI. LangGraph Overview, 2026. URL `https://docs.langchain.com/oss/python/langgraph/overview`. Accessed September 2026.

Hyung-Chul Lee, Yoonsang Park, Soo Bin Yoon, Seong Mi Yang, Dongnyeok Park, and Chul-Woo Jung. Vitaldb, a high-fidelity multi-parameter vital signs database in surgical patients. *Scientific Data*, 9(1):279, 2022.

Bo Li, Yuanhan Zhang, Dong Guo, Renrui Zhang, Feng Li, Hao Zhang, Kaichen Zhang, Peiyuan Zhang, Yanwei Li, Ziwei Liu, et al. Llava-onevision: Easy visual task transfer. *arXiv preprint arXiv:2408.03326*, 2024.

Leerang Lim, Hyeonhoon Lee, Chul-Woo Jung, Dayeon Sim, Xavier Borrat, Tom J Pollard, Leo A Celi, Roger G Mark, Simon T Vistisen, and Hyung-Chul Lee. Inspire, a publicly available research dataset for perioperative medicine. *Scientific Data*, 11(1):655, 2024.

Chi Liu, Derek Li, Yan Shu, Robin Chen, Derek Duan, Teng Fang, and Bryan Dai. Fleming-r1: Toward expert-level medical reasoning via reinforcement learning. *arXiv preprint arXiv:2509.15279*, 2025.

Chang Han Low, Ziyue Wang, Tianyi Zhang, Zhu Zhuo, Zhitao Zeng, Evangelos B. Mazomenos, and Yueming Jin. Surgraw: Multi-agent workflow with chain of thought reasoning for robotic surgical video analysis. *IEEE Robotics and Automation Letters*, 11(4):4857–4864, 2026. doi: 10.1109/LRA.2026.3665443.

Naoki Miyaguchi, Koh Takeuchi, Hisashi Kashima, Mizuki Morita, and Hiroshi Morimatsu. Predicting anesthetic infusion events using machine learning. *Scientific reports*, 11(1):23648, 2021.

Bala G. Nair, Eilon Gabel, Ira Hofer, Howard A. Schwid, and Maxime Cannesson. Intraoperative clinical decision support for anesthesia: A narrative review of available systems. *Anesthesia & Analgesia*, 124(2):603–617, 2017. doi: 10.1213/ANE.0000000000001636.

Jungwoo Oh, Gyubok Lee, Seongsu Bae, Joon-myoung Kwon, and Edward Choi. Ecg-qa: A comprehensive question answering dataset combined with electrocardiogram. *Advances in Neural Information Processing Systems*, 36:66277–66288, 2023.

OpenAI. GPT-6 Astra model documentation, 2026. URL `https://developers.openai.com/api/docs/models/gpt-6-astra`.

Laura Pasin, Pasquale Nardelli, Margherita Pintaudi, Massimiliano Greco, Massimo Zambon, Luca Cabrini, and Alberto Zangrillo. Closed-loop delivery systems versus manually controlled administration of total iv anesthesia: a meta-analysis of randomized clinical trials. *Anesthesia & Analgesia*, 124(2):456–464, 2017.

Goverdhan D Puri, Preethy J Mathew, Indranil Biswas, Amitabh Dutta, Jayashree Sood, Satinder Gombar, Sanjeev Palta, Morup Tsering, PL Gautam, Aveek Jayant, et al. A multicenter evaluation of a closed-loop anesthesia delivery system: a randomized controlled trial. *Anesthesia & Analgesia*, 122(1):106–114, 2016.

Qwen Team. Qwen3.8-27B model card, 2026a. URL `https://huggingface.co/Qwen/Qwen3.8-27B`.

Qwen Team. Qwen3.5: Towards native multimodal agents, February 2026b. URL https://qwen.ai/blog?id=qwen3.5.

Rafael Rafailov, Archit Sharma, Eric Mitchell, Christopher D Manning, Stefano Ermon, and Chelsea Finn. Direct preference optimization: Your language model is secretly a reward model. *Advances in neural information processing systems*, 36:53728–53741, 2023.

WB Runciman, MT Kluger, RW Morris, AD Paix, LM Watterson, and RK Webb. Crisis management during anaesthesia: the development of an anaesthetic crisis management manual. *Quality and Safety in Health Care*, 14(3):e1–e1, 2005.

Muntaha Samad, Mirana Angel, Joseph Rinehart, Yuzo Kanomata, Pierre Baldi, and Maxime Cannesson. Medical informatics operating room vitals and events repository (mover): a public-access operating room database. *JAMIA open*, 6(4):ooad084, 2023.

Bernd Saugel, Wolfgang Buhre, Michelle S. Chew, Bernard Cholley, Mark Coburn, Barak Cohen, et al. Intra-operative haemodynamic monitoring and management of adults having noncardiac surgery: A statement from the european society of anaesthesiology and intensive care. *European Journal of Anaesthesiology*, 42(6):543–556, 2025. doi: 10.1097/EJA.0000000000002174.

Samuel Schmidgall, Rojin Ziaei, Carl Harris, Eduardo Reis, Jeffrey Jopling, and Michael Moor. Agentclinic: a multimodal agent benchmark to evaluate ai in simulated clinical environments. *arXiv preprint arXiv:2405.07960*, 2024.

Andrew Sellergren, Sahar Kazemzadeh, Tiam Jaroensri, Atilla Kiraly, Madeleine Traverse, Timo Kohlberger, Shawn Xu, Fayaz Jamil, Cían Hughes, Charles Lau, et al. Medgemma technical report. *arXiv preprint arXiv:2507.05201*, 2025.

Yan Shu, Chi Liu, Robin Chen, Derek Li, and Bryan Dai. Fleming-vl: Towards universal medical visual reasoning with multimodal llms. *arXiv preprint arXiv:2511.00916*, 2025.

Karan Singhal, Shekoofeh Azizi, Tao Tu, S Sara Mahdavi, Jason Wei, Hyung Won Chung, Nathan Scales, Ajay Tanwani, Heather Cole-Lewis, Stephen Pfohl, et al. Large language models encode clinical knowledge. *Nature*, 620(7972):172–180, 2023.

Charles Spearman. The proof and measurement of association between two things. *The American journal of psychology*, 100(3/4):441–471, 1987.

Kirsten R Steffner, Matthew Christensen, George Gill, Michael Bowdish, Justin Rhee, Abirami Kumaresan, Bryan He, James Zou, and David Ouyang. Deep learning for transesophageal echocardiography view classification. *Scientific Reports*, 14(1):11, 2024.

Weiyun Wang, Zhangwei Gao, Lixin Gu, Hengjun Pu, Long Cui, Xingguang Wei, Zhaoyang Liu, Linglin Jing, Shenglong Ye, Jie Shao, et al. Internvl3. 5: Advancing open-source multimodal models in versatility, reasoning, and efficiency. *arXiv preprint arXiv:2508.18265*, 2025a.

Xidong Wang, Shuqi Guo, Yue Shen, et al. Liveclin: A live clinical benchmark without leakage. In *International Conference on Learning Representations*, 2026. URL https://proceedings.iclr.cc/paper_files/paper/2026/hash/9f45b2d4ace7ae425e40c7c1d0d37e64-Abstract-Conference.html.

Zhonghai Wang, Jie Jiang, Yibing Zhan, Bohao Zhou, Yanhong Li, Chong Zhang, Baosheng Yu, Liang Ding, Hua Jin, Jun Peng, et al. Hypnos: A domain-specific large language model for anesthesiology. *Neurocomputing*, 624:129389, 2025b.

Marije Wijnberge, Bart F Geerts, Liselotte Hol, Nikki Lemmers, Marijn P Mulder, Patrick Berge, Jimmy Schenk, Lotte E Terwindt, Markus W Hollmann, Alexander P Vlaar, et al. Effect of a machine learning–derived early warning system for intraoperative hypotension vs standard care on depth and duration of intraoperative hypotension during elective noncardiac surgery: the hype randomized clinical trial. *Jama*, 323(11):1052–1060, 2020.

Anyi Xu, Bangcai Lin, Bing Xue, Bingxuan Wang, Bingzheng Xu, Bochao Wu, Bowei Zhang, Chaofan Lin, Chen Dong, Chenchen Ling, et al. Deepseek-v4: Towards highly efficient million-token context intelligence. *arXiv preprint arXiv:2606.19348*, 2026a.

Weiwen Xu, Hou Pong Chan, Long Li, Mahani Aljunied, Ruifeng Yuan, Jianyu Wang, Chenghao Xiao, Guizhen Chen, Chaoqun Liu, Zhaodonghui Li, et al. Lingshu: Generalist foundation model for unified multimodal medical understanding and reasoning. *IEEE Transactions on Pattern Analysis and Machine Intelligence*, 2026b.

Zihan Xu, Yanzhen Chen, Xiaocheng Zhang, Zhiting Fan, Weiqi Zhai, Hongxia Xu, and Zuozhu Liu. Longmedbench: Benchmarking medical agents for long-horizon clinical decision-making. *arXiv preprint arXiv:2607.09322*, 2026c.

An Yang, Anfeng Li, Baosong Yang, Beichen Zhang, Binyuan Hui, Bo Zheng, Bowen Yu, Chang Gao, Chengen Huang, Chenxu Lv, et al. Qwen3 technical report. *arXiv preprint arXiv:2505.09388*, 2025.

Z.ai. GLM-4.7-Flash model card, 2026. URL `https://huggingface.co/zai-org/GLM-4.7-Flash`.

Aohan Zeng, Xin Lv, Qinkai Zheng, Zhenyu Hou, Bin Chen, Chengxing Xie, Cunxiang Wang, Da Yin, Hao Zeng, Jiajie Zhang, et al. Glm-4.5: Agentic, reasoning, and coding (arc) foundation models. *arXiv preprint arXiv:2508.06471*, 2025a.

Zhitao Zeng, Zhu Zhuo, Xiaojun Jia, Erli Zhang, Junde Wu, et al. Surgvlm: A large vision-language model and systematic evaluation benchmark for surgical intelligence, 2025b.

Hongbo Zhang, Junying Chen, Feng Jiang, Fei Yu, Zhihong Chen, Guiming Chen, Jianquan Li, Xiangbo Wu, Zhang Zhiyi, Qingying Xiao, et al. Huatuogpt, towards taming language model to be a doctor. In *Findings of the association for computational linguistics: EMNLP 2023*, pp. 10859–10885, 2023.

Ming Zhang, Yujiong Shen, Zelin Li, Huayu Sha, Binze Hu, Yuhui Wang, Chenhao Huang, Shichun Liu, Jingqi Tong, Changhao Jiang, et al. Llmeval-med: A real-world clinical benchmark for medical llms with physician validation. *arXiv preprint arXiv:2506.04078*, 2025.

Bohao Zhou, Yibing Zhan, Zhonghai Wang, Yanhong Li, Chong Zhang, Baosheng Yu, Liang Ding, Hua Jin, Weifeng Liu, Xiongbin Wang, et al. Benchmarking medical llms on anesthesiology: A comprehensive dataset in chinese. *IEEE Transactions on Emerging Topics in Computational Intelligence*, 9(4):3057–3071, 2025.

Lianghui Zhu, Xinggang Wang, and Xinlong Wang. Judgelm: Fine-tuned large language models are scalable judges. In *International Conference on Learning Representations*, volume 2025, pp. 51257–51296, 2025.

Yuxin Zuo, Shang Qu, Yifei Li, Zhangren Chen, Xuekai Zhu, Ermo Hua, Kaiyan Zhang, Ning Ding, and Bowen Zhou. Medxpertqa: Benchmarking expert-level medical reasoning and understanding. *arXiv preprint arXiv:2501.18362*, 2025.

# APPENDIX

**A. Dataset Construction and Annotation** . . . . . 16

*A.1. Data Sources and Harmonization* . . . . . 16

*A.2. Clinical Terminology* . . . . . 16

*A.3. Decision Anchors and Episodes* . . . . . 16

*A.4. Expert Annotation and Dataset Statistics* . . . . . 16

**B. Task Definitions and Evaluation Criteria** . . . . . 19

*B.1. Task Taxonomy* . . . . . 19

*B.2. Perception Metrics and Clinical Triplet Matching* . . . . . 19

*B.3. Clinical Rubrics and Score Aggregation* . . . . . 20

**C. AnesTRACE-Eval Training and Validation** . . . . . 21

*C.1. Evaluator Data and Clinical Evidence* . . . . . 21

*C.2. Training Configuration* . . . . . 22

*C.3. Agreement with Anesthesiologists* . . . . . 23

**D. Experimental and Agent Protocols** . . . . . 24

*D.1. Model Inventory and Runtime Configuration* . . . . . 24

*D.2. Inference Protocols and Prompt Templates* . . . . . 24

*D.3. Agent Framework, Memory, and Tools* . . . . . 24

*D.4. Agent Behavior and Efficiency Metrics* . . . . . 25

**E. Complete Experiments Results** . . . . . 26

*E.1. Intraoperative Perception Results* . . . . . 26

*E.2. Single-point Decision-Making Results* . . . . . 26

*E.3. Multi-step Decision-Making Results* . . . . . 26

**F. Ablation and Performance Analysis** . . . . . 27

*F.1. Model Scale and Domain Specialization* . . . . . 27

*F.2. Dimension-wise Performance Analysis* . . . . . 27

*F.3. Perception–Reasoning Bottleneck Analysis* . . . . . 28

*F.4. Quality–Efficiency Trade-offs* . . . . . 29

*F.5. Models performance in Different Surgical Subgroup* . . . . . 30

*F.6. Error Analysis for Decision-Making Tasks* . . . . . 31

**G. Qualitative Case Study** . . . . . 31

# A Dataset Construction and Annotation

## A.1 Data Sources and Harmonization

AnesTRACE derives patient states from four open-source datasets: VitalDB, MOVER, INSPIRE, and EchoNet-TEE (Lee et al., 2022; Samad et al., 2023; Lim et al., 2024; Steffner et al., 2024). L1 uses data from VitalDB, MOVER-SIS, and EchoNet-TEE; L2 uses VitalDB; and L3 uses linked VitalDB–INSPIRE records and MOVER-EPIC.

For VitalDB–INSPIRE alignment, we exactly match INSPIRE `operations.csv.case_id` to VitalDB `caseid`, yielding 2,594 locally verifiable linked cases. Procedure start aligns VitalDB seconds with INSPIRE minutes:

$$t^{\mathrm{INSPIRE}} = t_{\mathrm{op}}^{\mathrm{INSPIRE}} + \frac{t^{\mathrm{VDB}} - t_{\mathrm{op}}^{\mathrm{VDB}}}{60}. \tag{7}$$

We retain only temporally valid records within each procedure interval and treat INSPIRE as low-frequency perioperative context rather than second-level observations. Cases are included only when the clinical context, timeline, evidence, and recorded actions can be reliably reconstructed from information available at the decision point; invalid linkage, insufficient coverage, unresolved units, artifacts, and hindsight-dependent references are excluded. Dataset-specific parsers map records into the unified $(C, M, O)$ representation while preserving missing or conflicting values. For L3, trajectories are serialized as ordered turns, with references and future information removed before inference. Released task files contain only de-identified identifiers and relative time, and translation preserves all structured clinical values and metadata.

## A.2 Clinical Terminology

Table 7 summarizes the recurring medical terms represented in our AnesTRACE-Bench. Terms occurring in at least five records were retained after normalizing case, spelling, and close synonyms; closely related concepts were combined to keep the glossary compact.

## A.3 Decision Anchors and Episodes

A decision anchor $t_k$ marks a clinically relevant reassessment point. Its visible state is $S_k = (C, M_{t_k}, O_{W_k^{\mathrm{obs}}})$, with $W_k^{\mathrm{obs}} = [t_k - \Delta_{\mathrm{obs}}, t_k)$ restricted to prior evidence. Persistent abnormalities, phase transitions, and newly available tests define an initial pool of 5,017 candidate anchors and more than 9,000 multimodal instances. The final benchmark units are selected from this pool after artifact screening, temporal validation, and expert review. L2 exposes information available at or before T0, while L3 releases observations turn by turn. Future states, references, and screening labels remain hidden.

An L3 episode is an ordered segment of one recorded surgical trajectory (Bynum et al., 2014; Culwick et al., 2020; Runciman et al., 2005). After each response, the next recorded state is released without simulating the effect of the model's recommendation. L1 tests perception from TEE, waveforms, and trends; L2 tests diagnosis, risk, intervention, and reassessment at one anchor; L3 tests repeated state assessment and management as evidence evolves. References specify required elements, acceptable alternatives, and severe errors rather than one wording.

L3 provides six runner-bound context tools for patient profile, procedure/anesthesia context, medication state, the preceding intervention, visible tests, and episode memory, plus four knowledge tools. Full-tool runs expose the same inventory to each evaluated model, whereas per-turn budgets are fixed by the inference profile as detailed in Appendix D.3. Tools cannot query another patient or future state, and all calls and failures are logged.

## A.4 Expert Annotation and Dataset Statistics

After collecting and preprocessing records from the source datasets, we constructed candidate annotation instances using deterministic temporal and clinical filtering rules. DeepSeek-v4-Pro was used to generate candidate questions and responses for each instance (Xu et al., 2026a).

Table 7: Clinical terms and abbreviations used throughout AnesTRACE-Bench.

| **Clinical term** | **Definition** |
|---|---|
| *Physiological measurements and monitoring* | |
| ASA physical status | Preoperative classification of systemic health status. |
| TEE | Transesophageal echocardiography for intraoperative cardiac imaging. |
| ECG | Electrocardiographic recording of cardiac electrical activity. |
| HR | Heart rate, reported as beats per minute. |
| MAP | Mean arterial pressure over one cardiac cycle. |
| $SpO_2$ | Peripheral oxygen saturation estimated by pulse oximetry. |
| $EtCO_2$ | Carbon-dioxide partial pressure measured at end-expiration. |
| $FiO_2$ | Fraction of oxygen in the inspired gas mixture. |
| RR | Respiratory rate, reported as breaths per minute. |
| PIP | Peak pressure reached in the airway during inspiration. |
| PEEP | Positive pressure maintained at end-expiration. |
| Tidal volume | Gas volume delivered or exhaled during one breath. |
| Minute ventilation | Total gas volume ventilated per minute. |
| CVP | Central venous pressure measured near the right atrium. |
| Cardiac index | Cardiac output normalized to body-surface area. |
| BIS | Processed electroencephalographic index of hypnotic depth. |
| Arterial blood gas | Blood analysis of oxygenation, ventilation, and acid–base status. |
| Lactate | Blood marker associated with anaerobic metabolism and impaired perfusion. |
| *Anesthetic and vasoactive medications* | |
| Propofol | Intravenous hypnotic used to induce or maintain general anesthesia. |
| Remifentanil | Ultra-short-acting opioid used for intraoperative analgesia. |
| Fentanyl | Opioid analgesic used as part of perioperative anesthesia. |
| Sevoflurane / desflurane | Volatile inhalational anesthetics used to maintain anesthesia. |
| Rocuronium | Non-depolarizing neuromuscular blocker. |
| Norepinephrine | Catecholamine vasopressor used to support arterial pressure. |
| Phenylephrine | $Alpha_1$-adrenergic vasopressor that increases vascular tone. |
| Epinephrine | Adrenergic agonist with inotropic and vasopressor effects. |
| Ephedrine | Mixed-acting sympathomimetic used to increase blood pressure. |
| Vasopressin | Non-catecholamine vasopressor that increases vascular tone. |
| Dobutamine | Predominantly $beta_1$-adrenergic inotrope that increases cardiac output. |
| Esmolol | Ultra-short-acting $beta_1$-adrenergic blocker. |
| Atropine | Antimuscarinic agent commonly used to treat bradycardia. |
| Nitroglycerin | Vasodilator that predominantly reduces venous tone and preload. |
| TCI / MAC | Target-controlled infusion and minimum alveolar concentration. |
| *Clinical conditions and diagnoses* | |
| Hypotension / hypertension | Abnormally low or high arterial pressure in clinical context. |
| Hypoxemia | Abnormally low oxygen level in arterial blood. |
| Hypercapnia | Abnormally elevated carbon-dioxide level in arterial blood. |
| Bradycardia / tachycardia | Abnormally slow or rapid heart rate in clinical context. |
| Arrhythmia | Abnormal cardiac rate or rhythm pattern. |
| Apnea / hypoventilation | Absent or inadequate ventilation. |
| Airway obstruction | Partial or complete blockage that impairs airflow. |
| Bronchospasm | Bronchial smooth-muscle constriction that increases airway resistance. |
| Rebreathing | Re-inhalation of exhaled gas containing carbon dioxide. |
| Pneumothorax | Air in the pleural space that may impair lung expansion. |
| Pulmonary embolism | Obstruction of pulmonary arterial flow by embolic material. |
| Hemorrhage | Acute blood loss that may compromise circulating volume. |
| Cardiac arrest | Cessation of effective cardiac activity and circulation. |
| Acidosis | Abnormally low blood pH. |
| Essential hypertension | Chronic arterial hypertension without a secondary cause. |
| Type 2 diabetes mellitus | Chronic disorder of insulin resistance and glucose regulation. |
| Asthma | Chronic inflammatory airway disease with reversible obstruction. |
| Obstructive sleep apnea | Recurrent upper-airway collapse during sleep. |
| Pneumonia | Infection and inflammation of pulmonary parenchyma. |
| Coronary artery disease | Atherosclerotic disease limiting coronary blood flow. |
| Heart failure | Inability of the heart to meet circulatory demand adequately. |
| Atrial fibrillation | Supraventricular arrhythmia with irregular atrial activation. |
| Lung cancer | Malignant neoplasm arising in the bronchus or lung. |
| *Anesthetic procedures and surgery types* | |
| General anesthesia | Drug-induced unconsciousness requiring anesthetic support. |
| Mechanical ventilation | Machine-delivered respiratory support using controlled settings. |
| Lobectomy / wedge resection | Removal of a pulmonary lobe or wedge of lung tissue. |
| Video-assisted thoracoscopic surgery | Minimally invasive thoracic surgery performed through ports. |
| Bronchoscopy | Endoscopic examination or treatment of the tracheobronchial tree. |
| Hepatectomy / liver transplantation | Liver resection or replacement with a donor liver. |
| Gastrectomy / esophagectomy | Surgical removal of part or all of the stomach or esophagus. |
| Colectomy / hemicolectomy | Removal of all or part of the colon. |
| Laparoscopy / laparotomy | Abdominal access through small ports or an open incision. |
| Coronary artery bypass grafting | Graft-based revascularization around coronary stenoses. |
| Partial nephrectomy | Removal of a renal lesion while preserving remaining kidney tissue. |

These candidates were presented to 11 anesthesiologists with varying levels of clinical experience, who reviewed, corrected, and finalized the annotations on the PAI-iTAG platform[2]. Specifically, the annotation team comprised 5 anesthesiologists with 1–3 years, 3 with 4–5 years, and 3 with more than 5 years of clinical experience. The team contributed 75 physician-hours across 5,659

[2]Alibaba Cloud PAI-iTAG: `https://www.aliyun.com/product/bigdata/learn/itag`.

Table 8: Annotation workload of the anesthesiologist team, with task-specific annotation counts and time requirements across AnesTRACE-Bench.

| Task | Annotations | Annotation time | Avg. time/item | Time/100 items |
|---|---|---|---|---|
| Level One – TEE | 1000 | 10 h | 0.60 min | 1 h |
| Level One – Waveform | 1000 | 7 h | 0.42 min | 0.70 h |
| Level Two | 2000 | 26 h | 0.78 min | 1.30 h |
| Level Three | 1659 | 32 h | 1.16 min | 1.93 h |
| **Total** | **5659** | **75** h | **0.80** min | **1.33** h |

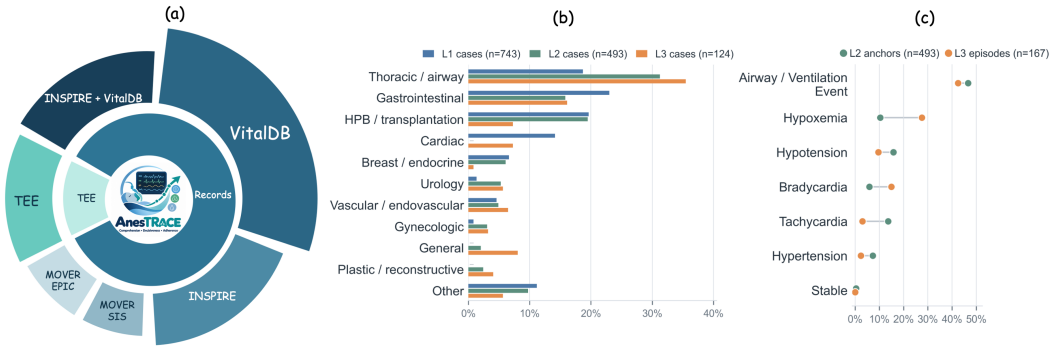


Figure 5: Data sources and distributions in AnesTRACE-Bench: (a) contributing data sources and modalities, (b) surgical-category distributions across the three levels, and (c) intraoperative event distributions in L2 and L3.

benchmark annotations, as summarized in Table 8. All final annotations were therefore determined by clinical experts rather than the generating model. The reviewed annotations were subsequently used to construct the benchmark and evaluator-training data.

Figure 5 summarizes the data sources and distributions of AnesTRACE-Bench. Panel (a) presents the contributing data sources and modalities, panel (b) compares the distribution of surgical categories across the three levels, and panel (c) shows the distribution of intraoperative events in L2 and L3. Thoracic/airway, gastrointestinal, and HPB/transplantation procedures account for substantial proportions of the surgical cases. The decision-oriented levels further cover a broad range of intraoperative events, including airway and ventilation events as well as hemodynamic and oxygenation abnormalities such as hypotension, hypoxemia, bradycardia, and tachycardia.

We complement these structured distributions by summarizing the clinical concepts represented in L2 and L3 in Figure 6.

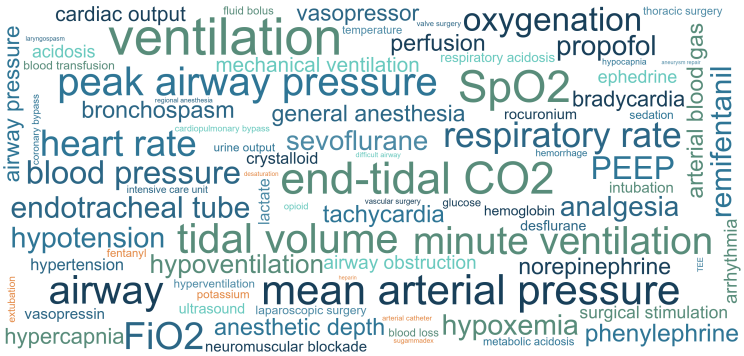


Figure 6: Concept cloud of frequently occurring clinical terms in AnesTRACE-Bench. Font size reflects term frequency.

Table 9: Comparison of medical and anesthesiology benchmarks. Temporal Updating denotes evaluation of management decisions as new patient information becomes available, rather than temporal perception alone. ✓ indicates explicit coverage, △ partial or supplementary coverage, and × that the capability is not an explicit evaluation target. Visual/Signal Input in AnesTRACE are assessed the performance that direct image, video, or physiological-signal representation are supplied to the model.

| **Benchmark** | **Anesthesia-Related Capabilities** | | | **Evaluation Dimensions** | | | | **Efficiency** |
|---|---|---|---|---|---|---|---|---|
| | **Intraoperative Decision** | **Physiological Waveform** | **TEE** | **Visual/Signal Input** | **Temporal Updating** | **Open-ended Management** | **Safety Evaluation** | **Response Latency** |
| *General medical perception* | | | | | | | | |
| GMAI-MMBench (Chen et al., 2024) | × | × | × | ✓ | × | × | × | × |
| OmniMedVQA (Hu et al., 2024) | × | × | × | ✓ | × | × | × | × |
| ECG-QA (Oh et al., 2023) | × | ✓ | × | ✓ | × | × | × | × |
| *General clinical evaluation and decision-making* | | | | | | | | |
| HealthBench (Arora et al., 2025) | × | × | × | × | × | ✓ | ✓ | × |
| LLMEval-Med (Zhang et al., 2025) | × | × | × | × | × | △ | ✓ | × |
| MIMIC-CDM (Hager et al., 2024) | × | × | × | × | △ | ✓ | △ | × |
| LiveClin (Wang et al., 2026) | × | × | × | ✓ | △ | × | × | × |
| AgentClinic (Schmidgall et al., 2024) | × | × | × | ✓ | △ | △ | × | × |
| MedAgentBench (Jiang et al., 2025) | × | × | × | × | × | △ | × | × |
| LongMedBench (Xu et al., 2026c) | × | × | × | × | ✓ | × | × | × |
| *Surgical visual benchmarks* | | | | | | | | |
| SurgVLM-Bench (Zeng et al., 2025b) | × | × | × | ✓ | × | × | × | × |
| SurgCoTBench (Low et al., 2026) | × | × | × | ✓ | × | × | × | × |
| *Anesthesiology benchmarks* | | | | | | | | |
| CAB (Zhou et al., 2025) | △ | × | × | × | × | △ | ✓ | × |
| Hypnos benchmark (Wang et al., 2025b) | △ | × | × | × | × | △ | ✓ | × |
| AnesBench (Feng et al., 2026) | △ | × | × | × | × | △ | × | × |
| **AnesTRACE (ours)** | ✓ | ✓ | ✓ | ✓ | ✓ | ✓ | ✓ | ✓ |

# B Task Definitions and Evaluation Criteria

We provide detailed task specifications for AnesTRACE-Bench in this section. Table 10 summarizes the tasks across its three levels, including their inputs, answer formats, scales, and evaluation dimensions. Table 9 compares AnesTRACE-Bench with existing medical, surgical, and anesthesiology benchmarks in terms of clinical scope, input modalities, temporal decision updating, safety evaluation, and response latency.

## B.1 Task Taxonomy and Input-Output Formats

Table 10 summarizes the task taxonomy, input–output formats, evaluation scales, and metrics across the three levels of AnesTRACE-Bench. L1 evaluates intraoperative perception from TEE and physiological waveforms, covering recognition, localization, functional assessment, and waveform understanding. L2 evaluates single-point anesthesia decision-making from clinical context and pre-decision physiological trends, with open-ended outputs for risk prediction, diagnosis, intervention, and reassessment. L3 extends this setting to longitudinal decision-making, conditioning each turn on the current state and preceding history and additionally evaluating consistency across the full decision trajectory.

## B.2 Perception Metrics and Clinical Triplet Matching

AnesTRACE-Bench uses task-specific evaluation metrics. Single-choice perception tasks are evaluated using accuracy. For a multiple selection question with reference set $Y_i$ and predicted set $\hat{Y}_i$, the sample-level Set-F1 is

$$\mathrm{SetF1}_i = \frac{2|Y_i \cap \hat{Y}_i|}{|Y_i| + |\hat{Y}_i|}. \tag{8}$$

The reported Set-F1 is the macro-average over questions. If both sets are empty, the score is defined as one; an invalid or missing prediction receives zero.

Table 10: Detailed three-level task hierarchy of AnesTRACE-Bench, including task inputs, answer formats, scales, and evaluation dimensions.

| Level | Input | Task Type | Answer Format | Scale | Evaluation Dimensions |
|---|---|---|---|---|---|
| L1 | TEE frame | Probe Position | Single choice | 82 | Accuracy |
| | TEE frame | Imaging Axis | Single choice | 79 | Accuracy |
| | TEE video | CFD Presence | Single choice | 30 | Accuracy |
| | TEE frame | Standard Imaging Plane | Single choice | 99 | Accuracy |
| | TEE frame | Structure Visibility | Single choice | 89 | Accuracy |
| | TEE frame | Structure Localization | Bounding box | 193 | mIoU |
| | TEE video | Assessability Judgment | Single choice | 80 | Accuracy |
| | TEE video | Functional Assessment | Labels + text | 83 | Accuracy; Factual-F1 |
| | TEE video | Abnormality Detection | Labels + text | 82 | Accuracy; Factual-F1 |
| | Waveform plot | Value Extraction | Single choice | 200 | Accuracy |
| | Waveform plot | Trend Recognition | Multiple selection | 400 | Set-F1 |
| | Waveform plot | Abnormality Detection | Structured response | 400 | Metric-F1 |
| L2 | Clinical context + pre-decision trends | Risk Prediction | Open-ended | 493 anchors | Clinical Correctness<br>Evidence Grounding<br>Task Completeness<br>Safety Error (B3/B4) |
| | | Clinical Diagnosis | Open-ended | | |
| | | Intervention Decision | Open-ended | | |
| | | Reassessment Plan | Open-ended | | |
| L3 | Current state + history | Turn-level Assessment and Intervention | Structured JSON | 517 turns | Clinical Correctness<br>Evidence Grounding<br>Task Completeness<br>Safety Error |
| | Recorded episode | Whole-trajectory Consistency | Decision sequence | 167 episodes | Temporal Evidence and Response Adaptation<br>Longitudinal Management Coherence |

Spatial grounding is evaluated using intersection over union:

$$\mathrm{IoU}_i = \frac{|B_i \cap \hat{B}_i|}{|B_i \cup \hat{B}_i|}, \qquad \mathrm{mIoU} = \frac{1}{N}\sum_{i=1}^{N} \mathrm{IoU}_i, \tag{9}$$

where $B_i$ and $\hat{B}_i$ are the reference and predicted bounding boxes.

Open-ended perception responses are represented as collections of atomic findings

$$\tau = (m, o, p), \tag{10}$$

where $m$ identifies a physiological metric or anatomical structure, $o$ denotes the associated observation or clinical finding, and $p$ indicates its presence state. We use task-specific projections of this representation. For TEE functional assessment and abnormality detection, *Factual-F1* matches all three fields after normalization. For waveform abnormality perception, *Metric-F1* matches the canonical metric identity $m$ only.

For each metric, matched findings count as true positives (TP), while unmatched predictions and references count as false positives (FP) and false negatives (FN), respectively:

$$\mathrm{F1}_i = \frac{2\mathrm{TP}_i}{2\mathrm{TP}_i + \mathrm{FP}_i + \mathrm{FN}_i}. \tag{11}$$

TEE Factual-F1 is macro-averaged over fact-scoring-eligible questions within each task; invalid or missing predictions receive zero. When an aggregate TEE Factual-F1 is reported, the functional-assessment and abnormality-detection task scores are averaged with equal weight. Metric and anatomical aliases are normalized before matching.

### B.3 Clinical Rubrics and Score Aggregation

AnesTRACE-Eval evaluates open-ended L2 and L3 responses against the patient information visible at the decision point, anesthesiologist-defined atomic criteria, the expert reference, and retrieved medical evidence. Patient-specific evidence is primary and references and external knowledge define acceptable clinical boundaries rather than a unique answer.

The five evaluation dimensions are defined in Table 11. The three turn-level ordinal dimensions apply to L2 and L3, safety is assessed for management outputs, and Temporal Consistency is evaluated only for complete L3 trajectories.

Table 11: Evaluation dimensions of AnesTRACE-Eval and their detailed definitions.

| **Dimension** | ***Definition*** |
|---|---|
| Clinical Correctness | *Evaluate the primary clinical conclusion and severity, together with the direction, priority, and key actions of the proposed management; a diagnosis or severity error that materially changes management, or a dangerous or contraindicated action, constitutes a decisive defect.* |
| Evidence Grounding | *Assess whether conclusions and actions follow from the available case evidence with appropriate temporal and causal reasoning, clinical prioritization, and calibration; unsupported claims, reversed evidence, unavailable information, and neglected relevant history are penalized.* |
| Task Completeness | *Examine whether all required content categories are present, including the diagnosis and its rationale or the required actions and plan details; factual or evidential errors are scored under the preceding dimensions rather than double-counted as missing content.* |
| Safety | *Identify avoidable harm arising from an unsafe action, consequential omission, inappropriate delay, dosing error, or failure to escalate, and classify its potential consequence as* safe*,* minor*,* major*, or* critical*.* |
| Temporal Consistency (L3) | *Determine whether later decisions incorporate new evidence and observed responses to recorded interventions, and whether management remains coherent by appropriately maintaining, escalating, de-escalating, or revising its strategy across turns.* |

Together, these dimensions assess response quality at the current decision point and, for L3, the coherence of decision updating across the trajectory.

We score each non-safety dimension on $\{0, 1, 2\}$. A score of 2 indicates that the response satisfies the relevant criteria without a clinically material defect; 1 indicates partial satisfaction with a bounded omission or imprecision; and 0 indicates a decisive error, unsupported conclusion, or failure to provide a required component.

Safety is reported separately as *safe*, *minor*, *major*, or *critical*. Because safety severity is not assumed to be linearly equivalent to the ordinal clinical dimensions, it is not converted into a compensatory numeric score. The principal safety outcome is the Major/Critical Safety Error Rate:

$$\text{Safety Error} = \frac{1}{N} \sum_{i=1}^{N} \mathbb{I}\left[ s_{\text{saf}}^{(i)} \in \{\textit{major}, \textit{critical}\} \right]. \tag{12}$$

The denominator includes only responses with a valid safety label. Missing or failed safety evaluations are excluded from this denominator and reported separately.

For each ordinal dimension $d$, model-level performance is reported as the mean over its scored evaluation units:

$$\bar{s}_d = \frac{1}{N_d} \sum_{i=1}^{N_d} s_{i,d}. \tag{13}$$

Ordinal scores are normalized to a 0–100 scale by multiplying the mean raw score by 50. The turn-level average equally weights Clinical Correctness, Evidence Grounding, and Task Completeness; Safety Error is reported separately. L2 uses decision anchors as evaluation units, whereas L3 uses individual decision turns. Dimension scores and Safety Error are reported separately so that a high average clinical score cannot obscure the frequency of serious safety errors.

# C AnesTRACE-Eval Training and Validation

## C.1 Evaluator Data and Clinical Evidence

AnesTRACE-Eval evaluates open-ended Level 2 and Level 3 responses. Each input contains the decision-point context, question, candidate response, atomic reference criteria, and, for Level 3, the preceding trajectory and newly revealed state. The scoring rubric is defined in Appendix B.3.

Table 12: Training configuration for AnesTRACE-Eval.

| **Hyperparameter** | **SFT** | **DPO** |
|---|---|---|
| Initialization | Qwen3.5-9B | SFT checkpoint |
| Fine-tuning | LoRA | LoRA |
| LoRA rank | 16 | 8 |
| LoRA $\alpha$ | 32 | 16 |
| LoRA dropout | 0.05 | 0.05 |
| LoRA target | All | All |
| Maximum sequence length | 8192 | 6144 |
| Per-device batch size | 2 | 1 |
| Gradient accumulation | 8 | 16 |
| Learning rate | 0.0001 | 0.000003 |
| Epochs | 3 | 1 |
| LR scheduler | Cosine | Cosine |
| Warmup ratio | 0.05 | 0.05 |
| Precision | BF16 | BF16 |
| Gradient checkpointing | Yes | Yes |
| Seed | 42 | 42 |
| DPO $\beta$ | – | 0.1 |
| Preference loss | – | Sigmoid |
| DeepSpeed | – | ZeRO-3 |

We use DeepSeek-V4-Pro to construct the initial evaluator-training data from benchmark cases, reference annotations, and the predefined evaluation rubric. The model generates candidate scores and rationales for SFT, as well as contrasting response pairs for preference annotation. All generated candidates are then reviewed, corrected, and formally annotated by anesthesiologists, with preference pairs additionally ranked by the experts. The resulting corpus contains approximately 7k expert-annotated SFT examples and 4k expert-ranked DPO (Rafailov et al., 2023) pairs.

The human-validation set is constructed separately from actual benchmark responses produced by five generator models whose outputs are excluded from evaluator training. Neither the validation responses nor outputs from these five generators are included in the SFT examples or DPO preference pairs. The validation models and sampling procedure are detailed in Appendix C.3.

For each case, a retrieval module supplies case-relevant passages from Miller's Anesthesia, ASA guidance, pharmacological references, and related literature. Retrieved passages are provided as auxiliary evidence to the evaluator; patient-specific observations visible at the decision point remain primary, and future-state information is excluded. The retriever is not treated as a separately fine-tuned clinical judge: SFT and DPO train Qwen3.5-9B to use the supplied evidence when producing rubric scores and rationales.

### C.2 Training Configuration

All experiments were conducted on 2 NVIDIA H100 80GB GPUs. SFT and DPO required approximately 17 and 2 hours of wall-clock time, corresponding to approximately 34 and 4 H100 GPU-hours, respectively. The complete settings are summarized in Table 12.

**Supervised fine-tuning.** Qwen3.5-9B is SFT-trained on approximately 7,000 reviewed examples using the settings in Table 12. Data are split at the patient or clinical-episode level, sequence packing is disabled, and checkpoints are saved every 50 optimizer steps.

Figure 7 shows the available logged SFT traces. The displayed loss is a logged/smoothed minibatch statistic. The downward loss trajectory and the absence of sustained gradient-norm growth indicate numerically stable optimization, but do not by themselves measure held-out clinical validity.

**Preference alignment.** Starting from the SFT checkpoint, DPO is applied to approximately 4,000 anesthesiologist-ranked pairs using the settings in Table 12.

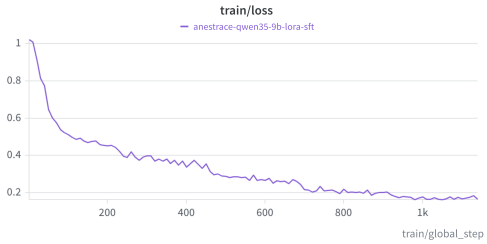


(a) SFT training loss

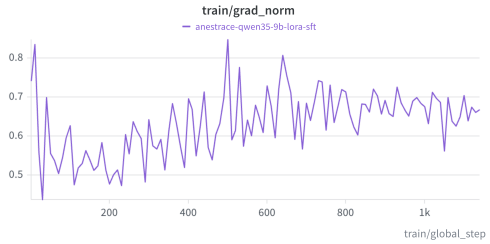


(b) SFT gradient norm

Figure 7: Optimization traces for supervised fine-tuning of AnesTRACE-Eval.

(a) Reward margin

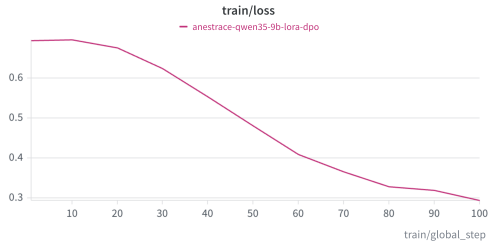


(b) DPO training loss

(c) Chosen reward

(d) Rejected reward

Figure 8: DPO optimization traces: (a) the reward margin, (b) training loss, (c) the chosen reward, and (d) the rejected reward.

The supplied DPO logs are visualized in Figure 8. Across the displayed 100 steps, the chosen reward increases, the rejected reward decreases, the reward margin expands to approximately 1.2, and the DPO loss declines from approximately 0.69 to 0.29. These trajectories show that the optimization objective separates the constructed preferred and rejected responses.

### C.3 Agreement with Anesthesiologists

We construct the human-validation set by sampling actual benchmark responses from five models: Fleming-R1-32B, GPT-OSS-20B, HuatuoGPT-3-32B, MedGemma-27B-text-it, and Qwen3.5-27B. These generators are held out from evaluator training: their outputs, including all sampled validation responses, are excluded from both SFT and DPO. The set contains 100 L2 responses and 117 L3 decision-turn responses from 39 episodes. Each L2 response includes the four clinical tasks, while L3 responses are reviewed within their corresponding episode context. Three anesthesiologists divide the annotation workload, with each item receiving one annotation under the same clinical rubric. These ratings provide the human reference for comparing the Base, SFT, and SFT+DPO evaluators.

Table 13 presents the agreement results from Table 5 separately for L2 and L3. We quantify agreement using Spearman's rank correlation coefficient (Spearman, 1987) and Kendall's $\tau_b$ (Kendall, 1945). Both measures generally improve after SFT and increase further after DPO across evaluation dimensions, including overall quality and safety assessment. These results show that AnesTRACE-

Table 13: Agreement of AnesTRACE-Eval variants with anesthesiologist ratings. Each cell reports Spearman's $\rho$ / Kendall's $\tau_b$. Overall aggregates Clinical Correctness, Evidence Grounding, and Task Completeness. Temporal Consistency applies only to L3.

| Level | Evaluator | Agreement with Anesthesiologist Ratings | | | | | |
|---|---|---|---|---|---|---|---|
| | | Clinical Correctness | Evidence Grounding | Task Completeness | Overall | Safety Severity | Temporal Consistency |
| L2 | Base | .46/.43 | .44/.41 | .39/.32 | .49/.42 | .38/.34 | – |
| | SFT | .57/.53 | .48/.45 | .50/.47 | .53/.45 | .48/.43 | – |
| | SFT + DPO | **.60/.56** | **.52/.49** | **.59/.54** | **.58/.50** | **.51/.47** | – |
| L3 | Base | .48/.44 | .35/.32 | .45/.38 | .47/.39 | .47/.41 | .37/.34 |
| | SFT | .68/.63 | .66/.62 | .46/.42 | .72/.62 | .77/.70 | .55/.52 |
| | SFT + DPO | **.71/.66** | **.69/.65** | **.68/.63** | **.75/.65** | **.80/.73** | **.58/.55** |

Eval achieves stronger agreement with anesthesiologist judgments after training, with both SFT and preference optimization contributing to the improvement.

# D Experimental and Agent Protocols

## D.1 Model Inventory and Runtime Configuration

For intraoperative perception tasks, we evaluate 16 MLLMs. The API-accessed models are GPT-6-Astra, Gemini 3 Pro Preview, Claude-Fable-5, and Qwen3.8-Max (OpenAI, 2026; Google, 2025; Anthropic, 2026; Alibaba Cloud, 2026). General-purpose open-weight models comprise Qwen3-VL-8B/32B (Bai et al., 2025), InternVL3.5-8B/38B (Wang et al., 2025a), LLaVA-OneVision-2-8B (Li et al., 2024), Qwen3.5-9B/27B (Qwen Team, 2026b), and Qwen3.8-27B (Qwen Team, 2026a). The medical-domain MLLMs are Lingshu-I-8B and Lingshu-32B (Xu et al., 2026b), and Fleming-VL-8B and Fleming-VL-38B (Shu et al., 2025).

For the decision-making tasks, we evaluate 19 LLMs. The API-accessed models include GPT-6-Astra, Gemini 3 Pro Preview, Claude-Fable-5, Qwen3.8-Max, and DeepSeek-V4-Pro (DeepSeek, 2026). General-purpose locally deployed models include Qwen3-8B (Yang et al., 2025), Qwen3.5-9B/27B (Qwen Team, 2026b), Qwen3.8-27B (Qwen Team, 2026a), GLM-4.7-Flash (Z.ai, 2026), and GPT-OSS-20B (Agarwal et al., 2025). Medical-domain models include Fleming-R1-7B/32B (Liu et al., 2025), HuatuoGPT-3-8B/32B (Chen et al., 2026), MedGemma-27B-text-it, Baichuan-M2-32B (Sellergren et al., 2025; Dou et al., 2025), and the anesthesia-specialized Morpheus-7B/32B (Feng et al., 2026).

Open-weight checkpoints are downloaded from their official Hugging Face repositories without task-specific adaptation and deployed on NVIDIA H100 GPUs in bfloat16 for inference. Locally deployed models use an OpenAI-compatible vLLM interface and API-accessed models are evaluated through their official API endpoints. We use temperature 0 where supported and fix local top-$p = 1$, top-$k = 0$, and seed 42, with explicit thinking disabled for compatible models.

## D.2 Inference Protocols and Prompt Templates

We present the model-facing prompts used at the three benchmark levels in the figures 11–13. Reference answers, hidden labels, and future information are excluded from every prompt.

## D.3 Agent Framework, Memory, and Tools

We implement L3 as a single-agent LangGraph workflow (LangChain AI, 2026). One graph invocation handles one decision point: turns are processed chronologically within an episode, while independent episodes can run concurrently. The initial prompt contains the procedure, decision time, and current vital-sign trends. The agent may alternate between model inference and tool execution before submitting a structured assessment and management recommendation. The graph then validates the response, attempts one format repair if needed, updates episode memory, and records the

Table 14: Tools available to the intraoperative agent. Patient-specific tools are restricted to the current turn.

| Tool Type | Tool | Data Source | Returned Information |
|---|---|---|---|
| Patient context | Patient profile<br>`get_patient_profile` | Current episode | Demographics, ASA status, and comorbidities. |
| | Procedure and anesthesia context<br>`get_procedure_anesthesia_context` | Current episode | Procedure, position, airway, and anesthesia context. |
| | Medication state<br>`get_anesthesia_medication_state` | Current turn | Active medications, infusion rates, and device settings. |
| | Previous intervention<br>`get_previous_intervention` | Previous turn | The preceding documented clinical intervention. |
| | Investigation results<br>`get_visible_test_results` | Current turn | Newly available laboratory and other test results. |
| Episode memory | Episode memory<br>`get_episode_memory` | Runtime memory | Prior agent assessments and recommendations. |
| External knowledge | Drug information<br>`get_anesthesia_drug_information` | RxNorm, openFDA | Drug labels, contraindications, and safety guidance. |
| | Clinical guidelines<br>`search_guidelines` | Local guideline corpus | Cited guideline passages and source metadata. |
| | Miller's Anesthesia<br>`search_miller_anesthesia` | Local textbook corpus | Cited passages with chapter and page information. |
| | PubMed literature<br>`search_pubmed` | NCBI PubMed | Article metadata and abstracts. |

turn result. Only after submission is the next recorded turn revealed; model-proposed actions do not alter the replayed trajectory.

Episode memory carries summaries of the agent's previous diagnoses and recommendations across turns and is reset between episodes. It is retrieved separately from the documented intervention at the preceding decision point. Thus, a prior recommendation is not treated as an executed action, and the agent can revise its assessment when new observations become available.

Table 14 lists the ten available tools. Five state-bound tools expose the patient profile, procedural and anesthesia context, current medication state, preceding documented intervention, and newly available test results; a sixth retrieves episode memory. These tools take no patient identifier or time-range arguments and return information scoped to the current episode or turn. Four knowledge tools accept model-generated drug names or queries to retrieve drug information, clinical guidelines, passages from *Miller's Anesthesia* (Gropper et al., 2024), and PubMed literature. Retrieved references can inform the recommendation but do not replace patient-specific observations. When the provided textual descriptions of visual observations are insufficient, the agent can invoke a supplementary visual perception tool backed by Qwen3.5-9B to extract additional information from the underlying visual inputs. Most evaluated models did not invoke this tool during the experiments.

The default per-turn budget permits at most six tool rounds and eight calls, including no more than six context calls and four knowledge calls. Each context tool can be called once per turn. Rejected calls and tool failures remain visible to the agent, while model requests, tool results, validation outcomes, and resource use are retained in the run traces.

### D.4 Agent Behavior and Efficiency Metrics

For L3, we measure agent behavior from execution traces separately from the clinical quality scores produced by AnesTRACE-Eval. Let $R_i$ denote the reference-related patient facts available at decision turn $i$, and let $A_i$ denote the facts recorded as acquired by the agent before its recommendation.

Table 15: Detailed L1 performance by perception task. All scores are reported as percentages, and higher values indicate better performance. Background colors denote model size: Small ($<$ 10B), Medium (10–40B), and Large ($>$ 40B).

| | Model | TEE | | | | | | | | | | | Waveform | | |
|---|---|---|---|---|---|---|---|---|---|---|---|---|---|---|---|
| | | Probe ACC | Axis ACC | CFD ACC | Plane ACC | Visibility ACC | Localization mIoU | Assessability ACC | Function ACC | Function Factual-F1 | Abnormality ACC | Abnormality Factual-F1 | Value ACC | Trend Set-F1 | Anomaly Metric-F1 |
| Proprietary MLLMs | GPT-6-Astra | 58.5 | 70.9 | 93.3 | 72.7 | 62.9 | 32.2 | 68.8 | 30.1 | 13.0 | 23.2 | 15.7 | 91.5 | 61.1 | 64.8 |
| | Gemini 3 Pro Preview | 69.5 | 67.1 | 93.3 | 56.6 | 46.1 | 24.6 | 46.3 | 27.7 | 13.5 | 29.3 | 12.7 | 77.0 | 62.6 | 54.8 |
| | Claude-Fable-5 | 70.7 | 75.9 | 93.3 | 68.4 | 64.2 | 23.4 | 42.7 | 40.1 | 27.8 | 35.5 | 26.0 | 80.5 | 68.7 | 59.6 |
| General Open-Weight MLLMs | Qwen3.8-MAX | 68.3 | 64.6 | 93.3 | 66.7 | 51.7 | 22.8 | 62.5 | 57.8 | 12.5 | 24.4 | 10.1 | 72.0 | 69.6 | 42.8 |
| | InternVL3.5-38B | 61.0 | 27.8 | 93.3 | 32.3 | 37.1 | 16.8 | 47.5 | 47.0 | 21.1 | 24.4 | 10.1 | 57.0 | 69.6 | 23.0 |
| | Qwen3-VL-32B | 52.4 | 49.7 | 93.3 | 46.8 | 32.3 | 18.2 | 23.6 | 45.9 | 7.6 | 41.5 | 6.4 | 55.0 | 71.7 | 28.6 |
| | Qwen3.5-27B | 36.6 | 59.5 | 93.3 | 44.4 | 43.8 | 18.9 | 43.8 | 56.6 | 16.8 | 29.3 | 10.7 | 56.0 | 65.3 | 36.5 |
| | Qwen3.8-27B | 58.5 | 48.1 | 93.3 | 34.3 | 33.7 | 14.8 | 42.5 | 51.8 | 9.3 | 39.0 | 14.2 | 57.5 | 72.5 | 31.3 |
| | Qwen3.5-9B | 59.8 | 30.4 | 93.3 | 33.3 | 52.8 | 15.5 | 40.0 | 57.8 | 8.8 | 28.0 | 6.2 | 54.5 | 60.7 | 33.1 |
| | Qwen3-VL-8B | 58.5 | 29.1 | 90.0 | 28.3 | 23.6 | 14.4 | 45.0 | 37.3 | 4.6 | 24.4 | 5.1 | 45.0 | 58.2 | 23.5 |
| | InternVL3.5-8B | 59.8 | 31.6 | 93.3 | 31.3 | 48.3 | 13.9 | 41.2 | 33.7 | 10.5 | 29.3 | 6.2 | 41.0 | 70.1 | 17.3 |
| | LLaVA-OneVision-2-8B | 54.9 | 30.4 | 90.0 | 24.2 | 50.6 | 14.3 | 32.5 | 47.0 | 1.6 | 31.7 | 4.9 | 49.5 | 60.6 | 23.6 |
| Medical Domain Open-Weight MLLMs | Fleming-VL-38B | 46.3 | 19.0 | 93.3 | 42.4 | 37.1 | 14.8 | 36.2 | 28.9 | 8.3 | 19.5 | 1.2 | 41.5 | 59.4 | 24.0 |
| | Lingshu-32B | 51.2 | 39.2 | 93.3 | 36.4 | 46.1 | 12.1 | 41.2 | 33.7 | 9.8 | 30.5 | 12.0 | 49.5 | 64.6 | 20.0 |
| | Lingshu-I-8B | 58.5 | 49.4 | 76.7 | 29.3 | 56.2 | 13.5 | 33.8 | 41.0 | 4.1 | 25.6 | 11.7 | 39.0 | 59.5 | 23.3 |
| | Fleming-VL-8B | 34.1 | 32.9 | 83.3 | 38.4 | 46.1 | 8.7 | 2.5 | 24.1 | 4.7 | 12.2 | 0.0 | 38.5 | 41.1 | 17.6 |

For turns with $|R_i| > 0$, Evidence Acquisition (EA) is reported at two aggregation levels:

$$\mathrm{EA}_{\mathrm{micro}} = \frac{\sum_{i \in \mathcal{I}} |A_i \cap R_i|}{\sum_{i \in \mathcal{I}} |R_i|}, \qquad \mathrm{EA}_{\mathrm{macro}} = \frac{1}{|\mathcal{I}|} \sum_{i \in \mathcal{I}} \frac{|A_i \cap R_i|}{|R_i|}, \tag{14}$$

where $\mathcal{I} = \{i : |R_i| > 0\}$. Micro EA measures aggregate reference-fact coverage and gives greater weight to turns with more reference facts; Macro EA gives each eligible decision turn equal weight. Because fact acquisition is determined by automatic matching, these metrics are proxies for information acquisition rather than physician-validated measures of clinically necessary evidence.

Invalid Tool Call Rate is the fraction of recorded calls that fail protocol or execution checks; budget-limit and duplicate-call rejections are tracked separately. Tool Calls / Turn is the mean number of recorded calls per decision turn. P95 Latency is the 95th percentile of recorded model-request time plus tool-execution time per turn. Output Tokens is the mean number of model-generated tokens per turn.

# E Complete Experiments Results

## E.1 Intraoperative Perception Results

We present disaggregates the L1 results in Table 3 by TEE and waveform task, reporting the corresponding task-level metrics.

## E.2 Single-point Decision-Making Results

We present the complete results of the two decision-making levels. Table 16 reports L2 performance for each of the four clinical tasks, disaggregated into clinical correctness, evidence grounding, and task completeness. Table 17 reports the corresponding results for MLLMs receiving paired-image inputs. Because the two tables use different input protocols, their scores are presented separately.

## E.3 Multi-step Decision-Making Results

For L3, Table 18 reports turn-level clinical scores, trajectory-level temporal consistency, and safety error rates. Table 19 complements these clinical outcomes with evidence acquisition, tool-use behavior, latency, and output-token consumption. Together, these tables separate the quality of sequential management recommendations from the information gathering and computational costs of the agent workflow.

Table 16: Detailed L2 performance by task and evaluation dimension. Clinical scores and Safety Error are reported as percentages; P95 Latency is reported in seconds. Background colors denote model size: Small (< 10B), Medium (10–40B), and Large (> 40B).

| | Model | Risk Prediction | | | Clinical Diagnosis | | | Intervention Decision | | | Reassessment Plan | | | Safety Error↓ | P95 Latency (s)↓ |
|---|---|---|---|---|---|---|---|---|---|---|---|---|---|---|---|
| | | Corr.↑ | Ground.↑ | Complete.↑ | Corr.↑ | Ground.↑ | Complete.↑ | Corr.↑ | Ground.↑ | Complete.↑ | Corr.↑ | Ground.↑ | Complete.↑ | | |
| Proprietary LLMs | GPT-6-Astra | 76.2 | 66.3 | 100.0 | 91.5 | 89.9 | 99.7 | 93.9 | 94.2 | 99.9 | 97.8 | 97.6 | 99.7 | 3.4 | 33.408 |
| | Gemini 3 Pro Preview | 64.6 | 51.8 | 97.0 | 66.9 | 60.4 | 96.7 | 58.6 | 57.2 | 90.8 | 81.5 | 81.5 | 95.3 | 13.5 | 26.946 |
| | Claude-Fable-5 | 86.2 | 76.2 | 98.8 | 90.1 | 86.8 | 98.8 | 82.5 | 82.0 | 98.8 | 95.5 | 95.9 | 97.4 | 9.4 | 39.964 |
| General Open-Weight LLMs | DeepSeek-V4-Pro | 72.9 | 61.6 | 100.0 | 78.7 | 72.1 | 99.7 | 71.7 | 69.1 | 96.1 | 91.9 | 91.7 | 97.8 | 14.8 | 14.040 |
| | Qwen3.8-Max | 61.9 | 51.7 | 98.4 | 73.0 | 67.5 | 98.2 | 61.7 | 60.5 | 92.7 | 83.5 | 83.2 | 95.9 | 15.1 | 23.514 |
| | Qwen3.5-27B | 59.0 | 49.3 | 100.0 | 65.2 | 58.8 | 99.7 | 61.4 | 59.8 | 89.3 | 70.1 | 69.1 | 94.5 | 28.6 | 22.139 |
| | Qwen3.8-27B | 63.1 | 51.1 | 100.0 | 66.2 | 60.8 | 99.6 | 54.6 | 52.4 | 91.2 | 67.4 | 66.7 | 90.8 | 21.5 | 22.935 |
| | GPT-OSS-20B | 60.3 | 47.1 | 100.0 | 52.1 | 45.7 | 99.5 | 31.4 | 29.1 | 91.7 | 54.3 | 52.9 | 91.2 | 37.5 | 17.904 |
| | GLM-4.7-Flash | 41.9 | 33.8 | 99.9 | 40.7 | 36.1 | 98.9 | 26.5 | 23.9 | 87.8 | 49.3 | 47.4 | 82.5 | 48.2 | 36.615 |
| | Qwen3.5-9B | 53.7 | 42.1 | 100.0 | 58.7 | 51.5 | 99.7 | 41.8 | 39.2 | 90.1 | 63.6 | 63.1 | 89.1 | 27.7 | 15.181 |
| | Qwen3-8B | 40.9 | 33.6 | 100.0 | 31.2 | 26.5 | 99.0 | 18.5 | 14.8 | 79.4 | 40.1 | 39.1 | 73.1 | 57.6 | 24.501 |
| Medical Domain Open-Weight LLMs | Morpheus-32B | 38.1 | 27.0 | 100.0 | 27.5 | 23.8 | 99.9 | 16.0 | 14.0 | 95.1 | 43.4 | 41.4 | 89.1 | 56.9 | 20.305 |
| | Fleming-R1-32B | 51.5 | 40.2 | 100.0 | 48.9 | 43.1 | 99.7 | 30.3 | 27.0 | 82.0 | 56.8 | 56.8 | 87.4 | 37.6 | 14.551 |
| | HuatuoGPT-3-32B | 49.7 | 38.4 | 100.0 | 44.4 | 37.8 | 100.0 | 25.7 | 23.6 | 93.6 | 41.7 | 41.4 | 95.9 | 50.9 | 25.049 |
| | Baichuan-M2-32B | 41.0 | 32.8 | 100.0 | 46.5 | 40.2 | 99.2 | 28.7 | 25.4 | 90.5 | 36.8 | 34.7 | 83.0 | 42.1 | 75.099 |
| | MedGemma-27B-text-it | 52.7 | 41.6 | 99.8 | 45.3 | 39.4 | 98.8 | 25.1 | 22.0 | 77.3 | 52.4 | 50.2 | 87.3 | 43.7 | 12.443 |
| | HuatuoGPT-3-8B | 18.6 | 14.4 | 100.0 | 9.3 | 7.0 | 100.0 | 4.8 | 4.5 | 97.6 | 19.0 | 19.4 | 98.2 | 85.9 | 9.874 |
| | Morpheus-7B | 23.4 | 17.7 | 99.9 | 14.9 | 12.0 | 99.9 | 10.9 | 9.6 | 96.4 | 32.6 | 30.9 | 87.7 | 67.4 | 26.802 |
| | Fleming-R1-7B | 34.9 | 30.2 | 99.9 | 32.2 | 25.8 | 99.5 | 13.6 | 12.2 | 95.6 | 41.9 | 40.2 | 83.6 | 59.0 | 9.193 |

Table 17: Detailed L2 performance for MLLMs with paired-image input. Clinical scores and Safety Error are reported as percentages; P95 Latency is reported in seconds. Background colors denote model size: Small (< 10B), Medium (10–40B), and Large (> 40B).

| | Model | Risk Prediction | | | Clinical Diagnosis | | | Intervention Decision | | | Reassessment Plan | | | Safety Error↓ | P95 Latency (s)↓ |
|---|---|---|---|---|---|---|---|---|---|---|---|---|---|---|---|
| | | Corr.↑ | Ground.↑ | Complete.↑ | Corr.↑ | Ground.↑ | Complete.↑ | Corr.↑ | Ground.↑ | Complete.↑ | Corr.↑ | Ground.↑ | Complete.↑ | | |
| General Open-Weight MLLMs | Qwen3-VL-32B-Instruct | 19.5 | 9.9 | 100.0 | 19.7 | 12.0 | 99.9 | 38.6 | 32.8 | 85.6 | 51.4 | 50.0 | 92.4 | 40.9 | 48.546 |
| | Qwen3.8-27B | 17.0 | 8.3 | 99.5 | 21.3 | 13.9 | 99.4 | 40.9 | 36.2 | 85.9 | 52.3 | 50.6 | 83.7 | 36.2 | 18.318 |
| | Qwen3.5-9B | 11.7 | 6.0 | 99.8 | 15.0 | 7.8 | 99.6 | 34.8 | 29.8 | 81.0 | 47.2 | 45.8 | 77.6 | 42.7 | 10.098 |
| | Qwen3-VL-8B-Instruct | 13.5 | 6.3 | 100.0 | 12.1 | 5.0 | 99.5 | 27.3 | 23.6 | 76.8 | 43.3 | 43.0 | 75.2 | 50.3 | 14.260 |
| | InternVL3.5-8B | 8.8 | 4.9 | 100.0 | 9.1 | 6.0 | 99.0 | 12.9 | 10.1 | 84.6 | 26.1 | 25.5 | 50.6 | 69.5 | 14.967 |
| Medical Domain Open-Weight MLLMs | Lingshu-32B | 13.2 | 10.6 | 99.9 | 15.2 | 11.7 | 99.3 | 16.6 | 13.7 | 78.0 | 33.5 | 32.9 | 52.7 | 66.8 | 26.080 |
| | Lingshu-I-8B | 5.0 | 3.8 | 100.0 | 5.6 | 3.0 | 98.7 | 4.0 | 2.7 | 90.0 | 13.7 | 13.5 | 49.0 | 88.4 | 6.597 |
| | Fleming-VL-8B | 11.6 | 7.8 | 59.4 | 18.1 | 14.8 | 60.4 | 19.3 | 18.6 | 54.2 | 29.9 | 29.5 | 41.2 | 66.8 | 17.099 |

# F Ablation and Performance Analysis

## F.1 Model Scale and Domain Specialization

Within individual model families, increasing model scale generally improves decision-making quality, although the gains are not uniform across all capabilities. For example, scaling Qwen3-VL from 8B to 32B improves waveform anomaly perception on L1, while Qwen3.5-27B substantially outperforms Qwen3.5-9B on both L2 average performance and L3 turn-level decision quality. However, improvements in overall clinical quality do not necessarily translate into better safety: despite the sizable gain in L2 average from Qwen3.5-9B to Qwen3.5-27B, the corresponding Safety Error Rate remains essentially unchanged (27.7 vs. 28.6).

And we also find that the evaluated medical-domain models do not show a consistent performance advantage over general-purpose models on AnesTRACE-Bench. For example, Qwen3.5-27B exceeds the anesthesia-specialized Morpheus-32B in both L2 average (73.0 versus 51.3) and L3 turn-level average (69.5 versus 46.2), and also outperforms Fleming-R1-32B (60.3 and 52.8, respectively). The pattern is not uniform: Fleming-R1-7B exceeds Qwen3-8B on both decision-making levels.

## F.2 Dimension-wise Performance Analysis

Across L2, *Evidence Grounding* is consistently the weakest clinical dimension for most model–task combinations (Table 16). This gap is especially apparent in *Risk Prediction*: for example, GPT-6-Astra achieves 0.762 in Clinical Correctness but only 0.663 in Evidence Grounding. This suggests that models may identify plausible short-term risks without adequately linking them to the physio-

Table 18: Detaidled L3 clinical decision performance. Clinical scores and Safety Error are reported as percentages. The three clinical dimensions average the corresponding diagnosis and intervention scores. Background colors denote model size: Small (< 10B), Medium (10–40B), and Large (> 40B).

| | Model | Turn-level Clinical Scores | | | | Temporal Consistency↑ | Safety Error↓ |
|---|---|---|---|---|---|---|---|
| | | Clinical Correctness↑ | Evidence Grounding↑ | Task Completeness↑ | Avg.↑ | | |
| Proprietary LLMs | GPT-6-Astra | 80.65 | 80.54 | 86.92 | 82.70 | 87.6 | 17.54 |
| | Gemini 3 Pro Preview | 63.23 | 60.70 | 74.31 | 66.08 | 78.01 | 38.52 |
| | Claude-Fable-5 | 76.07 | 79.27 | 82.54 | 79.40 | 82.5 | 24.3 |
| General LLMs | DeepSeek-V4-Pro | 77.52 | 74.85 | 87.65 | 80.01 | 81.92 | 19.17 |
| | Qwen3.8-Max | 64.63 | 58.41 | 78.34 | 67.13 | 85.33 | 40.09 |
| | Qwen3.5-27B | 66.16 | 61.80 | 80.61 | 69.52 | 81.59 | 32.50 |
| | Qwen3.8-27B | 62.81 | 60.52 | 74.91 | 66.08 | 69.16 | 34.05 |
| | GPT-OSS-20B | 53.12 | 49.13 | 68.91 | 57.05 | 67.22 | 53.41 |
| | GLM-4.7-Flash | 33.33 | 29.12 | 69.70 | 44.05 | 49.85 | 70.78 |
| | Qwen3.5-9B | 50.92 | 45.63 | 68.69 | 55.08 | 64.22 | 61.94 |
| | Qwen3-8B | 23.05 | 19.54 | 48.02 | 30.23 | 45.21 | 64.05 |
| Medical-Domain Open-Weight LLMs | Morpheus-32B | 36.86 | 29.98 | 71.78 | 46.21 | 55.99 | 66.02 |
| | Fleming-R1-32B | 48.77 | 43.53 | 66.20 | 52.83 | 66.87 | 56.52 |
| | HuatuoGPT-3-32B | 43.25 | 37.92 | 68.59 | 49.92 | 61.68 | 64.69 |
| | Baichuan-M2-32B | 40.40 | 36.94 | 71.20 | 49.51 | 56.14 | 66.67 |
| | MedGemma-27B-text-it | 45.14 | 41.67 | 59.41 | 48.74 | 54.34 | 59.41 |
| | HuatuoGPT-3-8B | 19.02 | 14.16 | 68.19 | 33.79 | 48.20 | 86.58 |
| | Morpheus-7B | 23.72 | 17.58 | 64.05 | 35.12 | 46.69 | 78.19 |
| | Fleming-R1-7B | 36.76 | 31.92 | 64.67 | 44.45 | 56.59 | 69.37 |

logical trends and patient-specific context available at the decision point. A second gap emerges between recognizing a clinical problem and selecting an appropriate intervention. Qwen3.5-9B scores 0.587 in diagnostic correctness but only 0.418 in intervention correctness, indicating that accurate state assessment does not necessarily translate into appropriate management.

The same flaw persists in L3, where *Evidence Grounding* remains lower than *Clinical Correctness* (Table 18); Qwen3.5-27B scores 61.80 versus 66.16, while GLM-4.7-Flash scores 29.12 versus 33.33. In the multi-step setting, however, grounding additionally requires integrating newly revealed observations with preceding clinical states and documented interventions, making failures of evidence integration more consequential as the episode evolves. *Temporal Consistency* captures a complementary trajectory-level weakness: models such as GLM-4.7-Flash (49.85) and Morpheus-7B (46.69) also struggle to maintain or appropriately revise management across successive decision points. These results indicate that correct local clinical judgments, evidence-grounded reasoning, and coherent longitudinal management remain distinct challenges for current models.

### F.3 Perception–Reasoning Bottleneck Analysis

We compare visual and structured textual representations for the same models and L2 cases (Fig. 2). All five paired models achieve higher decision quality with structured text, with average scores improving by 4.4–19.0 points and Safety Error Rates decreasing by 5.0–15.0 percentage points. The largest gap is observed for Qwen3.5-9B, whose average score increases from 46.3 to 65.3 while its Safety Error Rate decreases from 42.7% to 27.7%.

The complete results indicate that these gains are concentrated in clinical state interpretation and short-term risk assessment (Tables 17 and 16). For Qwen3.5-9B, structured text substantially improves both correctness and evidence grounding for *Risk Prediction* and *Clinical Diagnosis*, whereas the improvement in *Intervention Decision* correctness is comparatively modest (0.348 to 0.418). Notably, completeness for risk prediction and diagnosis is already near ceiling under visual input

Table 19: Detailed L3 agent behavior and efficiency. Evidence Acquisition and Invalid Call Rate are percentages. Evidence Acquisition automatically matches acquired reference-related patient facts and remains exploratory pending source-data version reconciliation. Output Tokens is the mean generated token count per turn. Background colors denote model size: Small ($<$ 10B), Medium (10–40B), and Large ($>$ 40B).

| | Model | Evidence Acquisition | | Tool Use | | Efficiency | |
|---|---|---|---|---|---|---|---|
| | | Micro↑ | Macro↑ | Invalid Call Rate↓ | Calls / Turn | P95 Latency (s)↓ | Output Tokens |
| Proprietary LLMs | GPT-6-Astra | 61.84 | 62.51 | 0.00 | 2.64 | 74.29 | 893.23 |
| | Gemini 3 Pro Preview | 74.44 | 76.36 | 0.00 | 3.30 | 101.37 | 2718.95 |
| | Claude-Fable-5 | 84.44 | 82.66 | 0.00 | 3.53 | 69.15 | 2944.37 |
| General Open-Weight LLMs | DeepSeek-V4-Pro | 89.74 | 87.88 | 0.05 | 4.03 | 14.41 | 508.54 |
| | Qwen3.8-Max | 62.84 | 61.95 | 0.00 | 2.07 | 22.87 | 674.32 |
| | Qwen3.5-27B | 83.30 | 84.13 | 0.00 | 4.00 | 34.38 | 535.21 |
| | Qwen3.8-27B | 86.92 | 85.57 | 0.00 | 4.01 | 39.88 | 567.01 |
| | GPT-OSS-20B | 59.49 | 60.97 | 0.00 | 2.86 | 106.55 | 1169.30 |
| | GLM-4.7-Flash | 95.44 | 97.18 | 0.00 | 7.03 | 63.60 | 554.91 |
| | Qwen3.5-9B | 89.54 | 90.93 | 0.00 | 3.63 | 27.22 | 792.89 |
| | Qwen3-8B | 32.7 | 34.8 | 0.00 | 0.71 | 10.29 | 539.72 |
| Medical-Domain Open-Weight LLMs | Morpheus-32B | 67.54 | 68.76 | 0.00 | 3.72 | 86.91 | 7118.69 |
| | Fleming-R1-32B | 11.33 | 15.11 | 0.00 | 1.76 | 22.80 | 521.56 |
| | HuatuoGPT-3-32B | 73.44 | 74.00 | 0.00 | 4.67 | 31.30 | 716.44 |
| | Baichuan-M2-32B | 95.98 | 96.63 | 0.00 | 7.01 | 32.98 | 558.96 |
| | MedGemma-27B-text-it | 40.49 | 42.96 | 0.00 | 1.11 | 34.37 | 457.87 |
| | HuatuoGPT-3-8B | 29.11 | 31.00 | 0.00 | 2.77 | 99.89 | 3548.53 |
| | Morpheus-7B | 8.32 | 6.70 | 0.00 | 0.44 | 50.40 | 3679.19 |
| | Fleming-R1-7B | 4.63 | 9.32 | 0.00 | 1.96 | 33.12 | 1280.85 |

(0.998 and 0.996), suggesting that the low clinical scores are not primarily caused by omitted response components, but by difficulty correctly interpreting and grounding the underlying physiological evidence. These results support the presence of an input-representation bottleneck: imperfect extraction of clinically relevant information from visual physiological inputs appears to substantially limit downstream state recognition and risk assessment.

### F.4 Quality–Efficiency Trade-offs

Figure 4 shows variation in decision quality and P95 Latency across the evaluated systems. Within the Qwen3.5 family, moving from 9B to 27B increases the L3 turn-level average from 56.6 to 69.1 and reduces Safety Error from 61.1% to 32.5%, while recorded P95 Latency rises from 27.2 to 34.4 seconds (Table 4). In this comparison, higher decision quality and fewer safety errors are accompanied by a modest increase in measured time per turn.

The complete agent results show that greater information acquisition or generation effort does not necessarily yield better management (Table 19). Baichuan-M2-32B records higher Evidence Acquisition than Qwen3.5-27B (96.0% versus 83.3%) and makes more tool calls per turn (7.01 versus 4.00). Despite similar P95 Latency (33.0 versus 34.4 seconds), its turn-level score is lower (49.5 versus 69.5) and its Safety Error Rate is higher (66.7% versus 32.5%). Output length is likewise not a proxy for clinical quality: HuatuoGPT-3-8B generates an average of 3,549 tokens per turn, compared with 716 for HuatuoGPT-3-32B, yet has lower turn-level quality (33.8 versus 49.9) and higher P95 Latency (99.9 versus 31.3 seconds). These comparisons motivate reporting clinical quality, safety, information acquisition, and computational cost as distinct outcomes. L3 latency sums recorded model-request and tool-execution times and is not directly comparable with the L2 response-time measure.

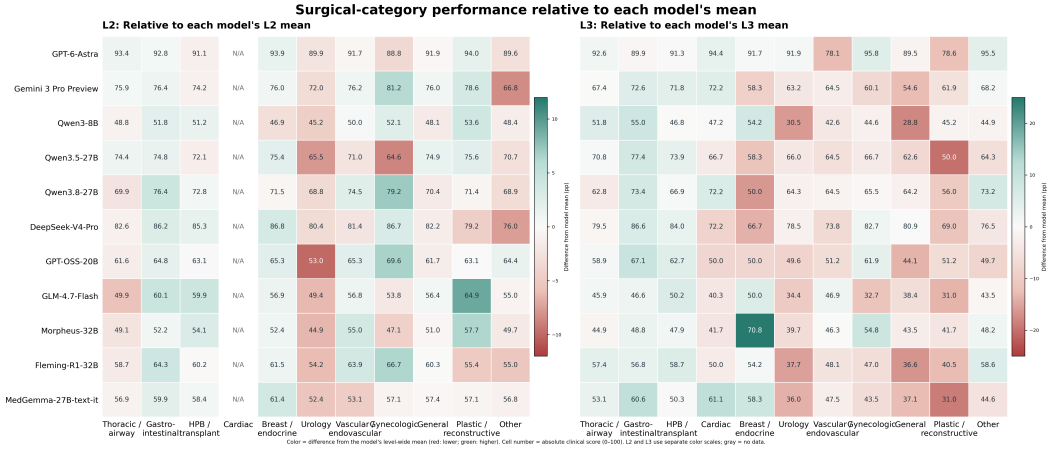


Figure 9: Performance across surgical categories in L2 and L3. Cell values show mean clinical scores (0–100). Colors indicate the difference, in percentage points, from each model's overall mean within the same level.

Table 20: **Error Summary**. Distribution of primary error categories across five representative models.

| Primary Error Category | GPT-6-Astra | DeepSeek-V4-Pro | Qwen3.5-27B | Qwen3.5-9B | Morpheus-32B |
|---|---|---|---|---|---|
| **L2: Single-Point Task Answers** | | | | | |
| Severity miscalibration | 45.4% | 24.2% | 24.1% | 21.4% | 17.5% |
| Problem misidentification | 11.8% | 20.6% | 19.3% | 17.9% | 33.1% |
| Inappropriate intervention | 4.0% | 10.4% | 15.8% | 18.1% | 18.4% |
| Observation misread | 7.0% | 15.5% | 11.4% | 15.6% | 14.9% |
| Unsupported evidence | 18.3% | 12.3% | 8.1% | 5.7% | 4.7% |
| Necessary action omitted | 2.8% | 9.6% | 8.3% | 9.6% | 5.3% |
| **L3: Turn-Level Task Answers** | | | | | |
| Severity miscalibration | 50.2% | 33.9% | 26.4% | 22.6% | 18.8% |
| Necessary action omitted | 23.3% | 22.4% | 20.5% | 21.6% | 15.1% |
| Inappropriate intervention | 1.8% | 8.7% | 16.0% | 22.3% | 24.2% |
| Problem misidentification | 6.8% | 9.6% | 12.6% | 13.0% | 20.8% |
| Observation misread | 4.6% | 8.3% | 10.2% | 9.9% | 11.4% |
| **L3: Episode-Level Temporal Errors** | | | | | |
| Longitudinal inconsistency | 40.6% | 28.3% | 34.7% | 33.1% | 40.5% |
| New evidence ignored | 28.1% | 41.3% | 34.7% | 37.8% | 32.4% |
| Prior action or response ignored | 6.2% | 13.0% | 15.3% | 17.3% | 14.2% |
| Escalation gap | 12.5% | 10.9% | 8.3% | 5.5% | 8.8% |
| Reassessment gap | 9.4% | 6.5% | 6.9% | 4.7% | 4.1% |

### F.5 Models performance in Different Surgical Subgroup

Figure 9 shows how clinical scores vary across surgical categories relative to each model's mean within the same level. In L2, urologic cases score below that mean for every model shown; the pattern persists for most models in L3. Plastic and reconstructive cases also receive lower relative scores in L3, whereas several models score above their respective means on gastrointestinal cases. For example, Qwen3.5-27B scores 77.4 on gastrointestinal cases but 50.0 on plastic and reconstructive cases in L3. Thus, aggregate scores obscure substantial variation across the surgical contexts represented in the benchmark. However, because subgroup sizes, case complexity, and clinical-event composition differ across categories, these results should be interpreted as evidence of subgroup-dependent performance variation rather than an intrinsic ranking of surgical difficulty.

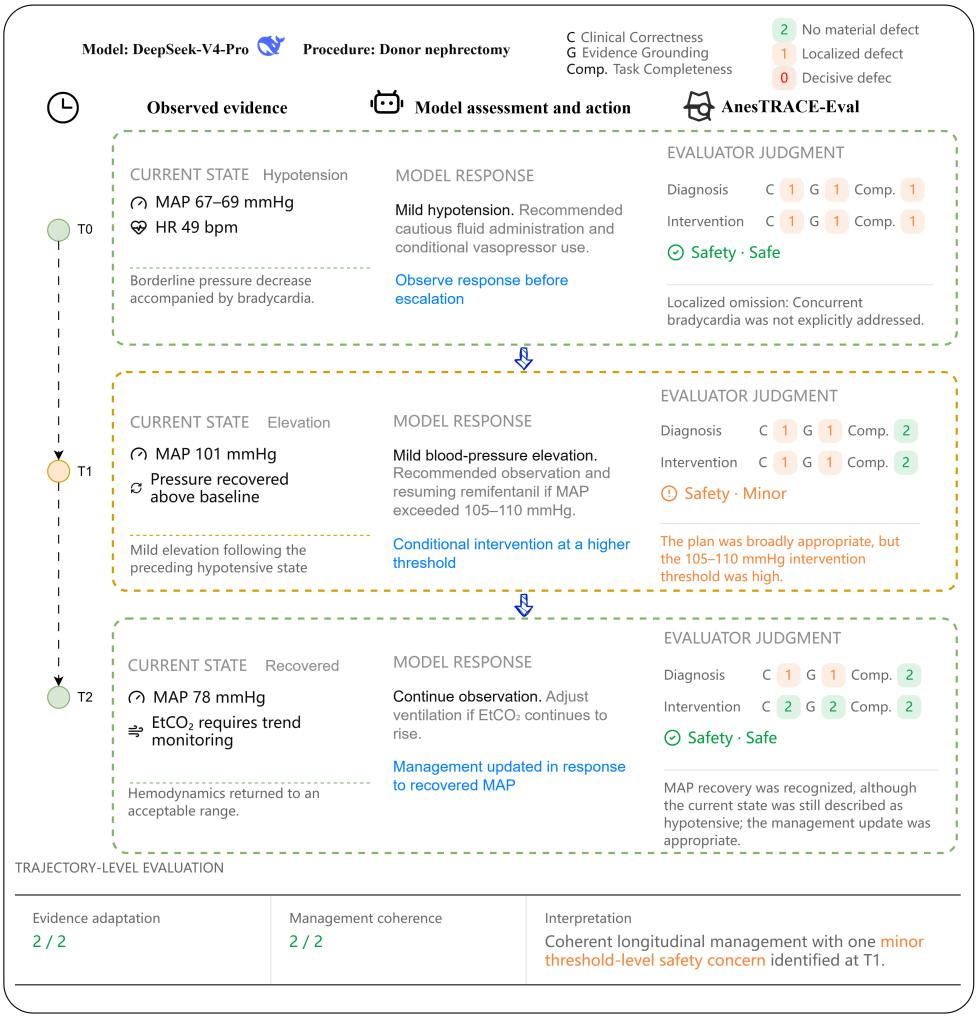


Figure 10: Turn- and trajectory-level evaluation of a representative L3 episode. DeepSeek-V4-Pro with full tools adapted its management across a donor-nephrectomy trajectory, while AnesTRACE-Eval identified localized turn-level defects and a minor safety concern at T1.

### F.6 Error Analysis for Decision-Making Tasks

To characterize decision-making failures, we analyze five representative models spanning proprietary, general-purpose, and medical-domain systems (Table 20). Among flagged units, two patterns recur: miscalibration of clinical severity and failure to update management as evidence evolves. In L2, severity miscalibration accounts for 17.5–45.4% of flagged answers; it is the largest category for GPT-6-Astra (45.4%), whereas problem misidentification is most frequent for Morpheus-32B (33.1%). In L3, severity miscalibration remains common at the turn level (18.8–50.2%). At the episode level, ignoring new evidence (28.1–41.3%) and longitudinal inconsistency (28.3–40.6%) account for substantial shares of flagged trajectories. These findings point to persistent difficulty in assessing clinical urgency and revising decisions across successive patient states.

## G Qualitative Case Study

**Representative Multi-step Episode**. Figure 10 illustrates the turn- and trajectory-level assessment of a three-turn donor-nephrectomy episode from the linked VitalDB–INSPIRE records. It aligns the evolving clinical evidence with the model's assessment and action at each turn, allow-

**L1: Multimodal perception.** The model receives the original TEE image or video, waveform, or trend plot and must answer using visible evidence only. The output contract is selected by task type: option identifier, spatial coordinates, or structured findings.

**Prompt used for L1 multimodal generation**

**SYSTEM PROMPT**

You are a medical visual analysis model trained in transesophageal echocardiography (TEE).

→ Answer using only the image or video currently provided.
→ Do not infer from filenames, paths, sample identifiers, or hidden metadata.
→ For candidate-based tasks, select only from the current question's options.
→ Do not fabricate structures, motion, flow, or abnormalities not visible in the input.
→ Output only the requested final answer; no Markdown, preamble, or chain-of-thought.

**MULTIMODAL USER INPUT**

[Original visual input] {TEE image | TEE video | waveform/trend image}
[Question] {question}
[Candidate options, when applicable] {option_id, option_text}

**TASK-SPECIFIC INSTRUCTION**

→ Choice tasks: identify probe position, imaging axis, CFD presence, standard view, structure visibility, or assessability.
→ Localization: locate the named structure and report its smallest reasonable normalized bounding box and center point.
→ Functional assessment: report assessability and all visible positive and negative structural, motion, and flow findings.
→ Abnormality detection: report only visible structural, motion, flow, effusion, mass, or device-related findings.

**OUTPUT CONTRACT**

```
Choice:
{"option_id":"A","text":"exact selected option text"}
Localization:
{"target_structure":"code","bbox":[x1,y1,x2,y2],"point":[x,y], [...]}
Functional assessment:
Assessability: assessable | limited | not assessable
Conclusion: {visible target-specific findings}
Abnormality detection:
Visually apparent abnormality: yes | no | uncertain | not assessable
Conclusion: {visible findings and imaging limitations}
```

Figure 11: Prompt used for L1 multimodal perception.

ing AnesTRACE-Eval to distinguish localized response defects from the coherence of the overall trajectory.

The retained L3 records include the observation, model response, turn-level rubric judgment, safety label, and trajectory-level assessment. Figure 10 presents a three-turn donor-nephrectomy episode from linked VitalDB–INSPIRE records, illustrating how AnesTRACE-Eval distinguishes localized defects from overall trajectory quality.

The evaluator considered the proposed management safe at T0 and T2, while identifying a minor concern at T1 because the proposed intervention threshold could delay treatment. Despite these localized defects, it assigned full scores to both evidence adaptation and management coherence across the trajectory. This example illustrates how turn-level rubric scores and safety labels complement trajectory-level assessment without reducing the episode to a single failure label.

**L2: Single-point clinical decision-making.** The prompt inserts the available patient state at one decision anchor and asks for one complete plan. Eight ordered sections separate risk, evidence, diagnosis, management, reassessment, and escalation without requiring JSON.

### Prompt used for L2 single-point clinical decision-making

**SYSTEM PROMPT**

You are an AI system performing intraoperative anesthesia decision-making.

→ Use only the current patient information supplied in the user message.
→ Do not invent unavailable laboratory results, imaging findings, medications, or clinical events.
→ Distinguish observed findings from possible etiologies and state uncertainty explicitly.
→ Account for missing, unreliable, or temporally misaligned measurements.
→ Prioritize the most clinically important current problem, patient safety, and actionable management.
→ Return clinical conclusions and supporting evidence without hidden reasoning.

**CURRENT PATIENT INFORMATION**

{{patient_information}}

**CLINICAL DECISION TASKS**

1. Risk Prediction — predict the single most important deterioration within the next 5 minutes.
   Predicted event · likelihood · severity · expected trajectory
2. Prediction Evidence — provide 1–4 temporally relevant measurements or trends.
3. Acute Diagnosis — identify the dominant current abnormality and most likely diagnosis.
   Current state and severity · most likely diagnosis · uncertainty when evidence is insufficient
4. Diagnostic Evidence — report the most relevant supporting and contradictory findings.
5. Management Decision — select the intervention level and immediate management goal.
6. Specific Actions — list prioritized actions, simultaneous checks, and conditional triggers.
7. Reassessment Plan — specify time, parameters, treatment target, and failure criteria.
8. Backup & Escalation Plan — define the next step and conditions for senior or emergency escalation.

**OUTPUT REQUIREMENTS**

【Risk Prediction】
【Prediction Evidence】
【Acute Diagnosis】
【Diagnostic Evidence】
【Management Decision】
【Specific Actions】
【Reassessment Plan】
【Backup & Escalation Plan】
Use exactly these headings and preserve their order.
Do not output JSON, reproduce the full input, or provide chain-of-thought.

Figure 12: Prompt used for L2 single-point clinical decision-making.

**L3: Tool-using sequential decision-making.** The initial prompt contains only the current partial observation. Bounded tools provide permitted context and external knowledge, and each turn ends with a structured state assessment and intervention in strict JSON.

### Prompt used for L3 tool-using sequential decision-making

**SYSTEM PROMPT**

You are an anesthesia decision agent reviewing a de-identified historical intraoperative trajectory.

→ The initial observation is deliberately partial.

→ Call only tools that are useful for the current decision; calling every tool is not required.

→ Do not invent information that a tool did not return.

→ Never request another patient, another episode, a future turn, future actions, future tests, or benchmark labels.

**HISTORY-SEPARATION RULES**

1. Previous intervention = an observed historical action, not proof of optimal care or causality.
2. Episode memory = prior model assessments and recommendations, not evidence that an action was executed.
3. Visible test results = findings newly available at the current turn; old abnormalities must not be carried forward without support.

**PER-TURN USER PROMPT**

```
[Current Procedure] {procedure_name}
[Current Decision Point] {T0–T4}
[Decision Time] {seconds from anesthesia/operation start; seconds from previous point}
[Vital-Sign Trends] {current trend observation}
[Task] {current clinical decision question}
```

**AVAILABLE TOOLS**

→ Context: patient profile; procedure/anesthesia context; medication state; previous intervention; visible tests; episode memory.

→ Knowledge: anesthesia drug information; clinical guidelines; *Miller's Anesthesia*; PubMed.

→ Retrieved knowledge may support mechanisms or treatment boundaries, but cannot establish a patient-specific fact.

**FINAL OUTPUT CONTRACT**

```
{
  "state_assessment": {
    "primary_problem": "...",
    "severity": "Stable|Mild|Moderate|Severe|Critical|Uncertain",
    "key_evidence": ["...", "..."]
  },
  "Specific_intervention": {
    "treatment_goal": "...",
    "action_list": [{"action_type":"...","decision":"..."}]
  }
}
```

**VALIDATION CONTROL**

→ If schema validation fails: repair JSON structure and allowed field values only; add no new clinical facts.

→ If the tool budget is exhausted: stop calling tools and answer from evidence already returned.

→ Output no preface, explanation, Markdown fence, or chain-of-thought outside the final JSON.

Figure 13: Prompt used for L3 tool-using sequential decision-making.